e-ISSN: 3023-6479

AOR

Volume: 3

Issue: 3

Year: 2026

Archives of Ophthalmological Research

MHA
MEDIHEALTH ACADEMY

Archives of
Ophthalmological Research

Editorial Board

Archives of
Ophthalmological Research

Editorial Board

Archives of
Ophthalmological Research

Editorial Board

Archives of
Ophthalmological Research

Contents

Volume: 3 Issue: 3 Year: 2026

ORIGINAL ARTICLES

Archives of
Ophthalmological Research

Original Article

DOI: 10.51271/AOR-0054

Iso-osmolar 5% mannitol for post-cataract corneal edema: efficacy and tolerability

Özgür Bülent Timuçin*, Yusuf Evcimen
Department of Ophthalmology, Van Training and Research Hospital, Van, Turkiye

Cite this article: Timuçin ÖB, Evcimen Y. Iso-osmolar 5% mannitol for post-cataract corneal edema: efficacy and tolerability. *Arch Ophthalmol Res.* 2026;3(3):41-46. doi:10.51271/AOR-0054

Received: 20/08/2026 ◆ **Accepted:** 21/09/2026 ◆ **Published:** 24/09/2026

ABSTRACT

Aims: To compare the efficacy and tolerability of topical iso-osmolar 5% mannitol with 10% mannitol and 5% sodium chloride (NaCl) for post-phacoemulsification corneal edema.

Methods: This prospective controlled study enrolled 81 patients with corneal edema after uncomplicated phacoemulsification. Patients received one of the three agents or control three times daily for 30 days. Central corneal thickness (CCT) was measured by Scheimpflug topography on postoperative days 5, 10, and 30. Day-30 tolerability was assessed on a 10-point Visual Analog Scale. Repeated-measures analysis of variance (ANOVA) and linear mixed-effects models (LMEMs) were used.

Results: CCT decreased significantly in all groups ($p<0.001$). ANOVA showed no overall treatment effect ($p=0.731$) or treatment×time interaction ($p=0.275$). In the LMEM, 5% mannitol was associated with lower postoperative CCT than control [$\beta=-5.83$ micrometers (μm); $p=0.001$] and 5% NaCl ($\beta=-4.15$ μm; $p=0.017$), but did not differ significantly from 10% mannitol ($p=0.463$). Comfort scores were higher with 5% mannitol than with 10% mannitol and 5% NaCl but did not differ significantly from control ($p=0.234$). Preoperative CCT predicted postoperative CCT ($\beta=0.94$; $p<0.001$); age and gender did not.

Conclusion: Iso-osmolar 5% mannitol was associated with lower postoperative CCT than control and 5% NaCl and greater comfort than the hyperosmotic comparators. However, nonsignificant overall treatment and interaction effects and no difference from 10% mannitol preclude superiority claims. Confirmation in larger studies including baseline endothelial cell density is required.

Keywords: Corneal edema, mannitol, sodium chloride, phacoemulsification, corneal pachymetry

INTRODUCTION

Rapid visual recovery following cataract surgery depends not only on surgical precision but also on the cornea's ability to quickly restore transparency. Corneal edema-most often related to endothelial stress and acoustic cavitation during phacoemulsification-is a common, usually self-limited complication.[1,2] While free radical development during surgery contributes to cellular injury,[3] the magnitude of this intraoperative endothelial insult is also modulated by surgical variables such as the ophthalmic viscosurgical device (OVD) employed; with contemporary dispersive agents, mean endothelial cell loss at one postoperative month remains in the range of 12-15%, without significant differences between formulations.[4] The resulting edema typically peaks within the first few days and subsides over 1-2 weeks.[5-7] However, the critical therapeutic window remains the first postoperative week, particularly in eyes with compromised endothelial function, where persistent swelling can delay visual rehabilitation.[8]

Traditionally, clinicians manage postoperative corneal edema with hyperosmotic topical agents such as 5% sodium chloride (NaCl; osmolality ~1700-1800 mOsm/kg) or 10% mannitol (~550 mOsm/kg).[5,9-11] These solutions aim to reduce stromal hydration by establishing a strong transepithelial osmotic gradient. However, such supraphysiologic osmolality has been associated with significant ocular surface discomfort, epithelial stress and pro-inflammatory signaling.[12,13] The literature suggests that hyperosmolar exposure can trigger a pro-inflammatory response [including cytokines such as interleukin (IL)-6, tumor necrosis factor (TNF)-α and IL-1β] and induce morphological changes in the corneal epithelium, which may inadvertently hinder the physiological recovery process and limit patient adherence.[13-16]

These clinical and tolerability challenges have prompted interest in the potential of iso-osmolar 5% mannitol (osmolality ~300 mOsm/kg). Unlike traditional agents that rely primarily on a dehydration-driven gradient, 5% mannitol

***Corresponding Author:** Özgür Bülent Timuçin, bulenttimucin@gmail.com

operates at near-physiologic osmolality. Beyond its osmotic properties, mannitol is a known hydroxyl radical scavenger that may exert antioxidant, anti-fibrotic and membrane-stabilizing effects.[17-19] Experimental and clinical models have suggested that mannitol can protect the endothelium from free-radical damage and support epithelial wound healing through specific signaling pathways.[20,21]

The primary aim of this study was to investigate whether clinical corneal recovery can be effectively managed-and potentially accelerated-by leveraging the proposed non-osmotic, cytoprotective properties of 5% mannitol. By comparing it with 10% mannitol and 5% NaCl using advanced statistical modeling, we sought to determine whether maintaining an iso-osmolar environment offers a favorable balance between CCT reduction and treatment tolerability.

METHODS

Ethics

This prospective, single-center trial adhered to the tenets of the Declaration of Helsinki (1975, revised in 2000) and was approved by the Van Training and Research Hospital Non-interventional Clinical Researches Ethics Committee (Date: 29.11.2024, Decision No: 60KAEK-2024-070). All participants provided written informed consent prior to inclusion.

Study Population

This study included 81 eyes of 81 patients who underwent phacoemulsification surgery. The inclusion criterion was the development of corneal edema following uncomplicated phacoemulsification. Patients were systematically assigned to one of four groups:

- 5% mannitol [prepared by 1:1 dilution of 10% mannitol (Terso; DMG, İstanbul, Turkiye) with sterile distilled water], administered three times daily (n=20). The diluted 5% mannitol was compounded by hospital pharmacy personnel under a sterile laminar-flow hood. The diluted formulation was stored at room temperature, with the bottle tightly closed and protected from heat sources, following the storage conditions specified for the commercial Terso product. Each prepared bottle was used for no longer than the 30-day study treatment period and was discarded at treatment completion.
- 10% mannitol (Terso; DMG, İstanbul, Turkiye), administered three times daily (n=21).
- 5% NaCl (Coredem; Deva Holding, İstanbul, Turkiye), administered three times daily (n=20).
- **Control:** Standard treatment consisting of topical antibiotics and steroids administered three times daily without any osmotic agent (n=20).

The treatments were administered for four weeks. Patients with preexisting corneal pathologies (e.g., corneal dystrophies or glaucoma) or a history of intraocular surgery were excluded. Additionally, individuals who experienced intraoperative or postoperative complications-such as Descemet membrane detachment, posterior capsule rupture, postoperative intraocular pressure elevation, toxic anterior segment syndrome, hypotony or wound leakage-were not included.

Surgical Technique

All surgeries were performed by a single experienced surgeon using the Stellaris Vision Enhancement System (Bausch & Lomb, Rochester, NY, USA). Procedures were standardized under topical anesthesia (0.5% proparacaine) and intracameral 1% lidocaine. A uniform superior clear-corneal main incision and two limbal paracenteses were used. Sodium hyaluronate (1.6 mg/ml) served as the OVD. Standard institutional preset parameters for vacuum, ultrasound and aspiration were maintained across all cases. Techniques included hydrodissection and hydrodelamination followed by nucleus emulsification.

Outcomes and Assessments

Treatment began on postoperative day 1 and continued for 30 days. The 30-day window was chosen to (i) capture the critical early recovery phase (days 1-10), when between-group differences are most likely; (ii) monitor the slower resolution observed in approximately 15-20% of cases;[8,22] and (iii) provide a uniform endpoint beyond the typical 2-week resolution to verify sustained normalization and safety.

- **Primary outcome:** The change in CCT from baseline to postoperative days 5, 10 and 30, measured with the Sirius Scheimpflug-Placido topographer (CSO, Florence, Italy).
- **Secondary outcome (treatment tolerability):** To assess the parallel impact of treatment on patient comfort, a VAS was used at postoperative day 30. Patients quantified their overall ocular comfort (considering stinging, burning or foreign body sensation) on a 10-point scale, where 0 indicated severe discomfort and 10 indicated complete comfort. To ensure objective data collection and minimize bias, the VAS assessment was performed by independent ophthalmology residents who were not members of the surgical team, had no involvement in treatment assignments and were not among the authors of this study. These evaluators remained completely masked to the study groups throughout the assessment period.
- **Other assessments:** Best-corrected visual acuity and intraocular pressure were also recorded.

Data Collection

The primary outcome of the study was the reduction in CCT over time, with the aim of identifying the treatment regimen that facilitated the most rapid resolution of corneal edema. Preoperative specular microscopy was not available; therefore, baseline endothelial cell density (ECD) was not captured.

Statistical Analysis

All data analyses (descriptive statistics, repeated-measures analysis of variance (ANOVA) and Bonferroni-corrected post-hoc tests) were conducted using JASP (version 0.19.1; JASP Team, University of Amsterdam, Amsterdam, The Netherlands). In addition, the LMEM was implemented in both Python (Statsmodels library, version 0.13.5; Python Software Foundation, Beaverton, OR, USA) and JASP to validate the robustness of the results across platforms. Post-hoc analyses were adjusted for preoperative CCT to account for baseline differences, providing conditional comparisons. Bonferroni correction was applied to control for multiple comparisons, and p-values less than 0.05 were considered statistically significant.

RESULTS

A total of 81 patients (81 eyes; mean age: 65.9±8.1 years; 44 males and 37 females) were evaluated across four treatment

groups: 5% mannitol (20 eyes), 10% mannitol (21 eyes), 5% NaCl (20 eyes) and control (20 eyes). CCT was measured on postoperative days 5, 10 and 30. Gender distribution did not differ significantly among the groups (p=0.890, Chi-square test). Age and preoperative CCT also did not differ significantly among groups (p>0.05, ANOVA). Visual acuity and intraocular pressure were recorded preoperatively and postoperatively, with no significant between-group differences (Table 1).

Table 1. Baseline demographic and preoperative characteristics of the study groups

Parameter	5% mannitol (n=20)	10% mannitol (n=21)	5% NaCl (n=20)	Control (n=20)	p-value
Age (years)	64.15±8.2	67.62±8.9	64.40±7.5	67.48±7.4	0.34¥
Gender (M/F)	10/10	12/9	10/10	12/9	0.90*
Preoperative CCT (µm)	533.35±22.3	537.43±36.3	537.15±36.0	540.38±26.9	0.82¥

Values are presented as mean±standard deviation unless otherwise stated. ¥One-way analysis of variance; *Chi-square test. Statistical significance was set at p<0.05. NaCl: Sodium chloride, M: Male, F: Female, CCT: Central corneal thickness, µm: Micrometers

Mixed-Effects Model: JASP Versus Python Comparison

A LMEM was applied via both JASP and Python to assess the effects of treatment and time on postoperative CCT. This analysis aimed to evaluate the consistency of findings across different statistical software programs and to ensure the reliability of the results.[22,23]

Preoperative CCT was identified as a strong and statistically significant predictor of postoperative CCT in both models. In the JASP analysis, the estimated effect of preoperative CCT was β=0.94±0.022 (p<0.001), whereas in Python the estimate was β=0.92±0.027 (p<0.001). These findings indicate that greater preoperative corneal thickness is associated with higher postoperative CCT values. The close agreement between both models underscores the robustness of this effect and highlights the critical role of preoperative CCT as a key determinant of postoperative corneal recovery.

The effect of postoperative time on CCT reduction was statistically significant in both models. In JASP, the mean difference in CCT between day 10 and day 5 was -14.528±0.683 micrometers (µm) (p<0.001), whereas the difference between day 30 and day 5 was -4.569±0.683 µm (p<0.001). In Python, the estimated mean difference in CCT between day 10 and day 5 was -18.33±1.447 µm (p<0.001), and between day 30 and day 5 it was -23.46±1.447 µm (p<0.001). Although both models confirmed a statistically significant reduction in CCT over time, Python's estimates suggested a greater decrease in CCT between days 10 and 30, whereas JASP's model indicated that CCT stabilized after day 10.

Treatment coefficient estimates differed slightly between the two models. In JASP, the 5% mannitol group had the largest numerical CCT estimate attributable to treatment (48.287±12.567 µm), followed by the 10% mannitol, 5% NaCl and control groups. In Python, with control as the reference, both mannitol concentrations were associated with lower postoperative CCT: 5% mannitol (β=-5.83 µm; p=0.001) and 10% mannitol (β=-4.55 µm; p=0.007). The 5% NaCl coefficient did not differ significantly from control (β=-1.68 µm; p=0.332).

Pairwise LMEM comparisons showed no statistically significant difference between 5% and 10% mannitol (β=-1.27 µm; p=0.463). The 5% mannitol group had lower postoperative CCT than the 5% NaCl group (β=-4.15 µm; p=0.017), whereas the 10% mannitol versus 5% NaCl comparison did not reach statistical significance (β=-2.88 µm; p=0.097). Thus, the LMEM indicates a modest association between 5% mannitol and lower postoperative CCT, but does not establish superiority, particularly in view of the nonsignificant overall treatment and treatment×time effects in the repeated-measures ANOVA.

Neither model identified age as a significant predictor of postoperative CCT. The p-value for age was 0.824 for JASP and 0.935 for Python, indicating that age does not significantly influence corneal thickness recovery. Gender showed a borderline effect in Python (p=0.075), suggesting a possible trend toward lower postoperative CCT values in males, although this finding was not statistically significant.

Overall, the findings from both JASP and Python confirm that preoperative CCT and postoperative time significantly influence corneal thickness recovery. While the general trends in treatment effectiveness were consistent, Python's model suggested a greater reduction in CCT over time, whereas JASP indicated a stabilization effect after day 10 (Figure 1).

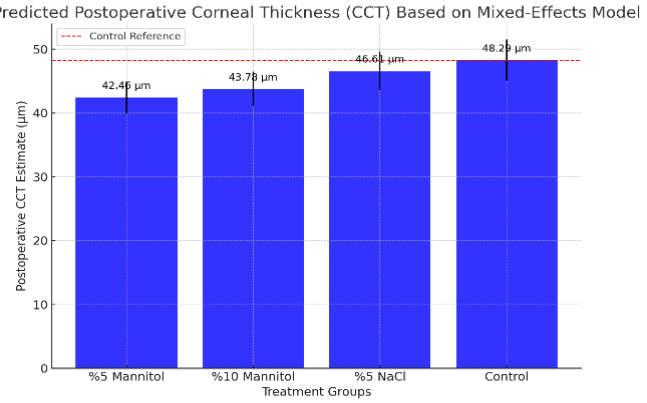

Figure 1. Postoperative CCT values according to the mixed-effects model estimates

CCT: Central corneal thickness; NaCl: Sodium chloride

Minor numeric discrepancies between JASP and Python primarily reflect implementation choices (e.g., optimizer algorithms, scaling methods and covariance structure specification) and differences in the coding of time contrasts. Both implementations yielded directionally consistent time effects and a similar numerical ranking of treatment estimates, with 5% mannitol showing the largest estimated reduction. This numerical ranking should not be interpreted as evidence of superiority.

Repeated-Measures ANOVA

Repeated-measures ANOVA revealed no significant difference between the treatment groups [F (3; 77)=0.432; p=0.731]. A significant reduction in corneal thickness was observed over time, particularly between day 5 and subsequent time points (p<0.001). The interaction effect between treatment and time

was not significant [F (3.25; 83.43)=1.314; p=0.275], indicating a similar recovery pattern across all groups.

Bonferroni-corrected post-hoc comparisons (time effect) were as follows. Day 5 vs. day 10; the mean difference in CCT was 19.117 µm (p<0.001), indicating a significant reduction in corneal thickness across all treatment groups during this period. Day 5 vs. day 30: the mean difference was 28.023 µm (p<0.001), indicating a further significant reduction in CCT by day 30. Day 10 vs. day 30; the mean CCT difference was 8.906 µm (p=0.077), suggesting that corneal thickness stabilized between these time points (Table 2). Between days 10 and 30, the overall recovery pattern remained consistent across all treatment groups, with no significant differences observed, indicating a plateau in corneal recovery after day 10 (Table 3, Figure 2).

Table 2. Estimated marginal means of postoperative CCT (µm) by treatment group and time point, derived from the linear mixed-effects model

Group	Postoperative day 5	Postoperative day 10	Postoperative day 30
5% mannitol	563.1 (SE=1.95)	542.6 (SE=0.67)	537.46 (SE=7.8)
10% mannitol	564.9 (SE=1.89)	543.6 (SE=0.65)	537.48 (SE=7.6)
5% NaCl	564.8 (SE=1.94)	545.6 (SE=0.67)	544.61 (SE=7.8)
Control	566.5 (SE=1.90)	551.0 (SE=0.66)	527.63 (SE=7.6)

All values are expressed in micrometers (µm). CCT: Central corneal thickness, NaCl: Sodium chloride, SE: Standard error

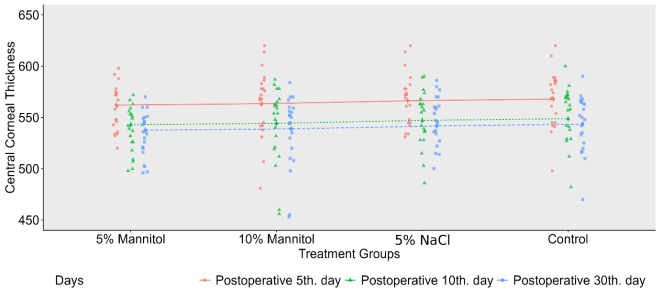

Figure 2. Changes in central corneal thickness across postoperative time points

NaCl: Sodium chloride

Patient Tolerability: VAS Comfort Scores

Parallel to the clinical recovery data, treatment tolerability was assessed at day 30 via a 10-point VAS. Significant differences in ocular comfort were observed between the groups (p<0.001, ANOVA).

- **5% mannitol vs. comparators:** The 5% mannitol group reported significantly higher comfort scores (7.13±0.79) than the 10% mannitol group (6.44±0.81; p=0.008) and the 5% NaCl group (5.78±1.07; p<0.001).
- **5% mannitol vs. control:** The comfort score in the 5% mannitol group (7.13±0.79) was not significantly different from that in the control group (6.85±0.70; p=0.234).
- **NaCl group:** The 5% NaCl group exhibited the lowest comfort scores among all groups, reflecting the irritation typically associated with high-osmolarity topical agents.

DISCUSSION

This study provides new evidence regarding the efficacy of three topical agents-5% mannitol, 10% mannitol, and 5% NaCl-in the treatment of corneal edema following phacoemulsification. The 5% mannitol group showed the greatest numerical reduction in central corneal thickness (CCT) during the early postoperative period, and the linear mixed-effects model (LMEM) estimated lower postoperative CCT values in this group than in the control and 5% NaCl groups. However, repeated-measures ANOVA showed no significant overall treatment effect or treatment×time interaction, and the LMEM analysis revealed no significant difference between 5% and 10% mannitol. Accordingly, the findings regarding the rate of corneal edema resolution should be interpreted as suggestive of a possible clinical effect rather than as evidence of unequivocal superiority of 5% mannitol.

The association between 5% mannitol and lower postoperative CCT despite its lower osmotic strength suggests that mechanisms beyond dehydration may contribute to this effect. Mannitol is a hydroxyl radical scavenger and can attenuate oxidative stress-related lipid peroxidation and cell

Table 3. Bonferroni-corrected pairwise comparisons of central corneal thickness between treatment groups at each postoperative time point

Time point	Group 1	Group 2	Mean difference (µm)	95% CI (lower-upper)	SE	pBonf	Significance
Postoperative day 5	5% mannitol	10% mannitol	-1.768	-9.126 to 5.590	2.717	1.000	ns
	5% mannitol	5% NaCl	-1.640	-9.112 to 5.832	2.759	1.000	ns
	5% mannitol	Control	-3.362	-10.740 to 4.015	2.724	1.000	ns
	10% mannitol	5% NaCl	0.128	-7.229 to 7.485	2.717	1.000	ns
	10% mannitol	Control	-1.594	-8.858 to 5.669	2.682	1.000	ns
	5% NaCl	Control	-1.722	-9.071 to 5.627	2.714	1.000	ns
Postoperative day 10	5% mannitol	10% mannitol	-1.032	-3.584 to 1.520	0.942	1.000	ns
	5% mannitol	5% NaCl	-3.016	-5.608 to -0.424	0.957	0.014	*
	5% mannitol	Control	-8.419	-10.978 to -5.860	0.945	<0.001	***
	10% mannitol	5% NaCl	-1.984	-4.535 to 0.568	0.942	0.231	ns
	10% mannitol	Control	-7.387	-9.906 to -4.867	0.930	<0.001	***
	5% NaCl	Control	-5.403	-7.952 to -2.854	0.941	<0.001	***
Postoperative day 30	5% mannitol	10% mannitol	-0.007	-29.504 to 29.490	10.892	1.000	ns
	5% mannitol	5% NaCl	-7.150	-37.105 to 22.805	11.061	1.000	ns
	5% mannitol	Control	9.831	-19.742 to 39.404	10.920	1.000	ns
	10% mannitol	5% NaCl	-7.143	-36.634 to 22.348	10.890	1.000	ns
	10% mannitol	Control	9.838	-19.279 to 38.956	10.752	1.000	ns
	5% NaCl	Control	16.981	-12.479 to 46.441	10.878	0.736	ns

*p<0.05, ***p<0.001. CI: Confidence interval, SE: Standard error, pBonf: Bonferroni-corrected p-value, NaCl: Sodium chloride, ns: Not significant

membrane damage. These properties support the possibility that, in addition to its osmotic activity, mannitol may exert antioxidant and cytoprotective effects on the cornea that facilitate edema resolution.[17,18] In experimental corneal models, mannitol-containing viscoelastic formulations have been shown to protect the endothelium against free radical-mediated injury,[20] while preoperative systemic mannitol administration has been associated with reduced endothelial cell loss after cataract surgery.[21] These mechanisms provide a biological rationale for the clinical trend observed in the present study. However, oxidative stress, apoptosis, and endothelial protection were not directly assessed; therefore, this explanation remains hypothesis-generating.

The tolerability findings were consistent with the near-physiological osmolality of 5% mannitol. Comfort scores were significantly higher in the 5% mannitol group than in the 10% mannitol and 5% NaCl groups, whereas no significant difference was observed compared with the control group. Because no non-inferiority margin or corresponding analysis was prespecified, the comparison with the control group indicates only the absence of a statistically significant difference and should not be interpreted as evidence of equivalence or non-inferiority. The better tolerability of 5% mannitol may be related to avoidance of the epithelial stress and stinging associated with hyperosmolar saline preparations.[12-15] Reduced ocular surface irritation may support treatment adherence during early recovery; however, adherence and epithelial integrity were not directly assessed in this study.

In the LMEM analysis, preoperative CCT was identified as a statistically significant predictor of postoperative CCT (β=0.941; $p<0.001$). Eyes with thicker corneas preoperatively had higher postoperative CCT values across all assessed time points. Nevertheless, this association is independent only with respect to the covariates included in the model and does not establish independence from unmeasured baseline ECD.

Baseline pachymetry may therefore provide useful prognostic information regarding postoperative CCT recovery within the scope of the variables measured in this study. However, pachymetry cannot substitute for specular microscopy, and adjustment for preoperative CCT cannot eliminate potential between-group differences in endothelial reserve. The observed association with CCT should therefore be interpreted as prognostic rather than as evidence that the treatment effect is independent of baseline ECD.

Pairwise between-group differences were most pronounced on postoperative day 10 and became less apparent by day 30. This finding suggests that any treatment-related separation may be concentrated in the early postoperative period.[5,6] However, because the treatment×time interaction was not significant, this temporal interpretation remains exploratory.

A strength of this study is the combined use of repeated-measures ANOVA and LMEM, with analyses performed in both JASP and Python.[22] The LMEM accounted for repeated observations and adjusted for measured variability in baseline CCT, an approach well suited to longitudinal ophthalmic data.[23,24] However, baseline ECD was not measured. Adjustment for preoperative CCT therefore cannot statistically eliminate unobserved differences in ECD or establish that the observed between-group differences in CCT represent a true treatment effect independent of endothelial reserve.

This single-center study had a relatively modest sample size and did not include baseline ECD measurements, standardized cataract grading, or case-level records of phacoemulsification energy and duration. Consequently, residual confounding related to baseline endothelial reserve and surgical energy exposure cannot be excluded. An identical dispersive viscoelastic protocol was used in all cases, and comparative evidence indicates similar endothelial cell loss among contemporary dispersive OVDs following uncomplicated phacoemulsification.[4] All procedures were performed by the same surgeon using the same platform, device settings, and incision technique. Participants and assessors were masked, visit windows and imaging protocols were standardized, and the LMEM was adjusted for baseline CCT. Future multicenter studies should prospectively collect specular microscopy data, standardized cataract grades, and case-level phacoemulsification energy and duration records. Dedicated stability studies should also be performed when compounded formulations are evaluated.

Limitations

This single-center study had a relatively modest sample size and did not include baseline ECD measurements, standardized cataract grading, or case-level records of phacoemulsification energy and duration. Consequently, residual confounding related to baseline endothelial reserve and surgical energy exposure cannot be excluded. Although all procedures were performed by a single surgeon using the same platform, preset parameters, incision technique, and dispersive viscosurgical protocol, these measures do not replace direct assessment of baseline ECD. Participants and outcome assessors were masked, visit windows and image acquisition were standardized, and the LMEM adjusted for baseline CCT; however, adjustment for CCT cannot eliminate unmeasured differences in endothelial reserve. The diluted 5% mannitol was compounded by the hospital pharmacy under a sterile laminar-flow hood and handled according to the commercial Terso instructions, but its stability after dilution was not independently tested. The findings should therefore be confirmed in larger multicenter studies incorporating baseline specular microscopy, standardized cataract grading, case-level phacoemulsification parameters, and dedicated stability testing of compounded formulations.

CONCLUSION

Iso-osmolar 5% mannitol was associated with lower postoperative CCT than the control and 5% NaCl groups in the LMEM, as well as higher comfort scores than the two hyperosmotic comparators. Nevertheless, repeated-measures ANOVA showed no significant overall treatment effect or treatment×time interaction, and the LMEM analysis revealed no significant difference between 5% and 10% mannitol. Preoperative CCT was identified as a significant prognostic covariate within the measured model. Larger studies incorporating baseline specular microscopy measurements are needed to confirm these findings.

ETHICAL DECLARATIONS

Ethics Committee Approval

This study was approved by the Van Training and Research Hospital Non-interventional Clinical Researches Ethics Committee (Date: 29.11.2024, Decision No: 60KAEK-2024-070).

Informed Consent

Written informed consent was obtained from all individual participants prior to their inclusion in the study. Participants were fully informed about the study's aims, procedures, potential risks and benefits, and their rights-including the right to withdraw at any time without consequence. All participants voluntarily signed a written informed consent form.

Peer Review Process

This manuscript was subject to external peer review.

Conflict of Interest

The authors declare no conflicts of interest related to this study.

Financial Disclosure

The authors received no financial support for the conduct or publication of this research.

Author Contributions

Concept: ÖBT, YE; Design: ÖBT, YE; Control: ÖBT, YE; Resources: ÖBT, YE; Materials: ÖBT, YE; Data Collection and/or Processing: ÖBT, YE; Analysis and/or Interpretation: ÖBT, YE; Literature Review: ÖBT, YE; Writing the Article: ÖBT, YE; Critical Review: ÖBT, YE.

Acknowledgments

The authors would like to thank the clinical residents of the ophthalmology department at the study institution for their diligent support, patient coordination and dedicated assistance in data management throughout the study period.

REFERENCES

1. Chen K, Xu WY, Sun SS, Zhou HW. Corneal endothelial cells and acoustic cavitation in phacoemulsification. *World J Clin Cases*. 2023;11(8):1712-1718. doi:10.12998/wjcc.v11.i8.1712
2. Geffen N, Topaz M, Kredy-Farhan L, et al. Phacoemulsification-induced injury in corneal endothelial cells mediated by apoptosis: in vitro model. *J Cataract Refract Surg.* 2008;34(12):2146-2152. doi:10.1016/j.jcrs.2008.08.024
3. Takahashi H. Free radical development in phacoemulsification cataract surgery. *J Nippon Med Sch*. 2005;72(1):4-12. doi:10.1272/jnms.72.4
4. Ataş M, Çiçek A, Ulusoy DM, et al. Comparison of the endothelial protective effect of two different dispersive viscoelastics during phacoemulsification surgery. *J Glouc Cat*. 2019;14(4):175-179.
5. Sabur H, Kabatas EU. Comparison of topical 5% NaCl versus 10% mannitol for the treatment of corneal edema after phacoemulsification. *Eur J Ophthalmol.* 2025;35(2):492-498. doi:10.1177/11206721241273631
6. Khripun KV, Nizametdinova Y, Varganova TS. Therapeutic efficacy of 3% NaCl hypertonic solution in postoperative corneal edema. *Ophthalmol J*. 2018;11(2):81-86. doi:10.17816/OV11281-86
7. Tzamalis A, Dermenoudi M, Diafas A, et al. Safety and efficacy of hypertonic saline solution (5%) versus placebo in the treatment of postoperative corneal edema after uneventful phacoemulsification: a randomized double-blind study. *Int Ophthalmol.* 2020;40(9):2139-2150. doi:10.1007/s10792-020-01395-4
8. Hayashi K, Yoshida M, Manabe S, Hirata A. Cataract surgery in eyes with low corneal endothelial cell density. *J Cataract Refract Surg.* 2011;37(8):1419-1425. doi:10.1016/j.jcrs.2011.02.025
9. Agrawal S, Gupta S, Gupta N, Vanathi M, Tandon R. Efficacy of hypertonic saline in treatment of corneal edema: a randomized crossover trial. *Med J Armed Forces India*. 2024;80(5):522-527. doi:10.1016/j.mjafi.2022.06.014
10. Ho Wang Yin G, Sampo M, Soare S, Hoffart L. Visual acuity, pachymetry and corneal density after 5% sodium chloride treatment in corneal edema after surgery. *J Fr Ophtalmol.* 2015;38(10):967-973. doi:10.1016/j.jfo.2015.07.002
11. Rouland JF. Clinical pilot study to evaluate the efficacy of a preservative-free hypertonic ophthalmic solution for patients with symptomatic corneal edema. *J Fr Ophtalmol.* 2015;38(9):800-808. doi:10.1016/j.jfo.2015.04.011
12. Schrage N, Wuestemeyer H, Langefeld S. Do different osmolar solutions change the epithelial surface of the healthy rabbit cornea? *Graefes Arch Clin Exp Ophthalmol.* 2004;242(8):668-673. doi:10.1007/s00417-004-0883-1
13. Prasad D, Siddiqui MG, Dar MAA, et al. Assessing the independent and combined effects of hyperosmolarity and inflammatory stress on human corneal epithelial cells. *Invest Ophthalmol Vis Sci.* 2025;66(13):47. doi:10.1167/iovs.66.13.47
14. Kontoh-Twumasi R, Aliste A, Scheid A, Glass J, Sharma A, Sharma S. L-carnitine partially restores adherens junction integrity and promotes wound healing in human corneal epithelial cells exposed to hyperosmolar stress. *Exp Eye Res.* 2025;258:110499. doi:10.1016/j.exer.2025.110499
15. Dutescu RM, Panfil C, Schrage N. Osmolarity of prevalent eye drops, side effects, and therapeutic approaches. *Cornea*. 2015;34(5):560-566. doi:10.1097/ICO.0000000000000368
16. Cha MJ, Cho H, Yeon Y, Kim YJ. Protective effects of miR-16-5p and miR-142-3p on inflammation and autophagy in human corneal epithelial cells under hyperosmotic stress in vitro. *Int J Mol Sci.* 2025;27(1):422. doi:10.3390/ijms27010422
17. Halliwell B. Antioxidants and human disease: a general introduction. *Free Radic Biol Med*. 2000;28(7):1200-1206.
18. Inaba K, Minami M, YamaguChi M, et al. Effects of the ophthalmic additive mannitol on antimicrobial activity and corneal toxicity of various preservatives. *Chem Pharm Bull (Tokyo).* 2020;68(11):1085-1091. doi:10.1248/cpb.c20-00540
19. Nagai N, Yoshioka C, Tanino T, Ito Y, Okamoto N, Shimomura Y. Decrease in corneal damage due to benzalkonium chloride by the addition of mannitol into timolol maleate eye drops. *J Oleo Sci.* 2015;64(7):743-750. doi:10.5650/jos.ess14275
20. Belda JI, Artola A, Garcia-Manzanares MD, et al. Hyaluronic acid combined with mannitol to improve protection against free-radical endothelial damage: experimental model. *J Cataract Refract Surg.* 2005;31(6):1213-1218. doi:10.1016/j.jcrs.2004.11.055
21. Hwang HS, Ahn YS, Cho YK. Preoperative mannitolization can decrease corneal endothelial cell damage after cataract surgery. *Curr Eye Res.* 2016;41(9):1161-1165. doi:10.3109/02713683.2015.1101138
22. Zhang H, Lu N, Feng C, et al. On fitting generalized linear mixed-effects models for binary responses using different statistical packages. *Stat Med*. 2011;30(20):2562-2572. doi:10.1002/sim.4265
23. Kutluturk Karagoz I, Keskin B, Özkalaycı F, Karagöz A. Linear mixed model better than repeated measures analysis. *Eur J Ophthalmol.* 2020;30(6):NP1-NP2. doi:10.1177/1120672119890518
24. Fan Q, Teo YY, Saw SM. Application of advanced statistics in ophthalmology. *Invest Ophthalmol Vis Sci.* 2011;52(9):6059-6065. doi:10.1167/iovs.10-7108

Archives of
Ophthalmological Research

Original Article

DOI: 10.51271/AOR-0055

Retinal safety and apoptotic effects of intravitreal nepafenac: an experimental rabbit study

Yaşar Ölmez*[1], Tevfik Oğurel[1], Nurgül Örnek[1], Zafer Onaran[1], Reyhan Oğurel[2]

[1]Department of Ophthalmology, Faculty of Medicine, Kırıkkale University, Kırıkkale, Turkiye
[2]Department of Ophthalmology, Oğurel Private Eye Clinic, Kırıkkale, Turkiye

Cite this article: Ölmez Y, Oğurel T, Örnek N, Onaran Z, Oğurel R. Retinal safety and apoptotic effects of intravitreal nepafenac: an experimental rabbit study. *Arch Ophthalmol Res.* 2026;3(3):47-51. doi:10.51271/AOR-0055

Received: 28/06/2026 ◆ **Accepted:** 21/09/2026 ◆ **Published:** 24/09/2026

ABSTRACT

Aims: To evaluate the clinical, histopathological, and apoptotic effects of intravitreal administration of nepafenac, a non-steroidal anti-inflammatory drug, on healthy rabbit retinas.

Methods: Forty-two New Zealand white rabbits were included in this experimental study. The eyes were divided into three groups: a control group (n=10), a low-dose intravitreal nepafenac group (0.05 mg/ml, n=16), and a high-dose group (0.1 mg/ml, n=16). Clinical ophthalmological examinations were performed at baseline, 1 week, and 1 month after injection. Eyes were enucleated at predefined time points (week 1 or month 1) for histopathological evaluation using hematoxylin-eosin staining. Apoptotic cell death was assessed using the terminal deoxynucleotidyl transferase-mediated dUTP nick end labelling (TUNEL) method.

Results: No statistically significant differences were observed between groups in terms of intraocular pressure or central corneal thickness at any time point ($p>0.05$). Transient lens opacities were observed in 6 eyes (4 in the high-dose group and 2 in the low-dose group) during the first week after injection; these resolved completely by the first month. Histopathological examination revealed preserved retinal layer integrity in all groups. TUNEL analysis demonstrated no significant difference in Apoptotic Index between the control and treatment groups ($p>0.05$).

Conclusion: Intravitreal nepafenac administration did not result in significant histopathological or apoptotic toxicity in healthy rabbit retinas in the short and medium term. These findings suggest that nepafenac may represent a potential intravitreal anti-inflammatory agent; however, further studies evaluating repeated dosing and diseased models are required before clinical application.

Keywords: Intravitreal injection, nepafenac, retinal toxicity, apoptosis, TUNEL analysis

INTRODUCTION

Macular edema is one of the important causes of vision loss that can develop after diabetic retinopathy, uveitis, retinal vascular diseases, and cataract surgery. Current studies have shown that inflammatory mediators and prostaglandin pathways play an important role in the pathogenesis of macular edema. Therefore, anti-inflammatory therapies are among the basic approaches in the management of macular edema.[1-4]

Today, intravitreal corticosteroids are widely used in the treatment of macular edema due to their strong anti-inflammatory effects. However, serious side effects of these drugs, such as cataract development and increased intraocular pressure, limit their long-term use.[5-8] This situation increases the need for alternative treatment options that have similar anti-inflammatory efficacy but a safer side effect profile.

Non-steroidal anti-inflammatory drugs (NSAIDs) suppress inflammation by inhibiting the cyclooxygenase pathway in arachidonic acid metabolism, thereby reducing prostaglandin synthesis.[9] In ophthalmology, topical NSAIDs are widely used for indications such as controlling inflammation and preventing cystoid macular edema after cataract surgery.[10] However, it is debatable whether topical applications achieve sufficient drug concentrations in the posterior segment due to the blood-retina barrier.[11]

Nepafenac is a non-steroidal anti-inflammatory prodrug that rapidly converts to its active metabolites in ocular tissues.[12] Topical nepafenac use has been shown to reduce the risk of cystoid macular edema and control inflammation after cataract surgery.[13-16] However, the literature on intravitreal application of NSAIDs, and especially nepafenac, is limited, and data on the retinal safety profile are insufficient.

***Corresponding Author:** Yaşar Ölmez, yolmez01@gmail.com

METHODS

Ethics

The study protocol was approved by the Kırıkkale University Experimental Animal Ethics Committee (Date: 25.02.2016, Decision No: 16/35). All procedures were carried out in accordance with the Association for Research in Vision and Ophthalmology (ARVO) principles on the use of animals in vision and ophthalmology research, the ARRIVE guidelines, and relevant national and international guidelines for the care and use of laboratory animals.

Experimental Animals

In this experimental study, 42 eyes of 42 healthy adult New Zealand white rabbits weighing between 2.5-3.0 kg were used. All animals were kept under standard laboratory conditions (12-hour light/12-hour dark cycle, room temperature 22±2°C) and fed with standard rabbit feed throughout the experiment.

Study Groups

Experimental animals were randomly divided into three groups:

- **Control group (10 rabbits):** Eyes receiving intravitreal balanced salt solution (BSS) as a sham injection
- **Group 1 (16 rabbits):** Eyes with intravitreal 0.1 mg/ml nepafenac injection
- **Group 2 (16 rabbits):** Eyes with intravitreal 0.05 mg/ml nepafenac injection

The control eyes received the same volume of intravitreal BSS using the same injection technique and procedure as the nepafenac-treated eyes, thereby serving as the sham-injection control group.

Intravitreal Injection Procedure

All injection procedures were performed under sterile conditions. Rabbits were given general anesthesia with intramuscular ketamine hydrochloride (35 mg/kg) and xylazine (5 mg/kg). Pupillary dilation was achieved with topical tropicamide 1%. Conjunctival antisepsis was performed with 5% povidone iodine. Intravitreal injections were administered approximately 2.5-3.0 mm posterior to the limbus, in the superior temporal quadrant, using a 30-gauge needle. The control eyes received intravitreal BSS, whereas the treatment eyes received nepafenac at the doses specified in the study protocol (Figure 1).

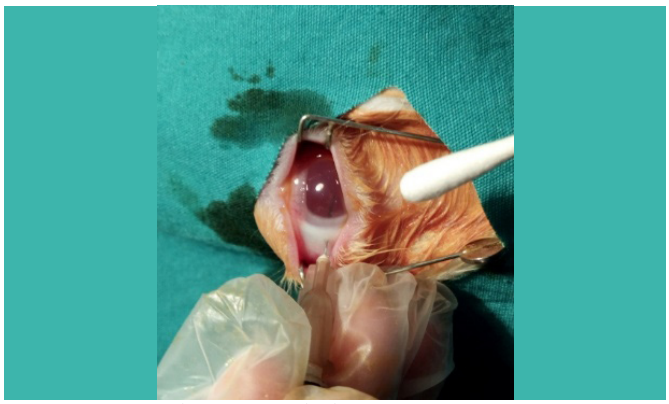

Figure 1. Intravitreal injection method

Clinical Ophthalmological Evaluation

All rabbits underwent basic clinical examination methods, including slit-lamp biomicroscopy, direct ophthalmoscopy, pachymetry (Reichert), and intraocular pressure assessment (Tono-pen), before injection and at 1 week and 1 month after injection, before sacrifice (Figure 2). The cornea, anterior chamber, and lens in the anterior segment; and the vitreous and retina structures in the posterior segment were examined for inflammation, opacity, and other possible complications (Table 1).

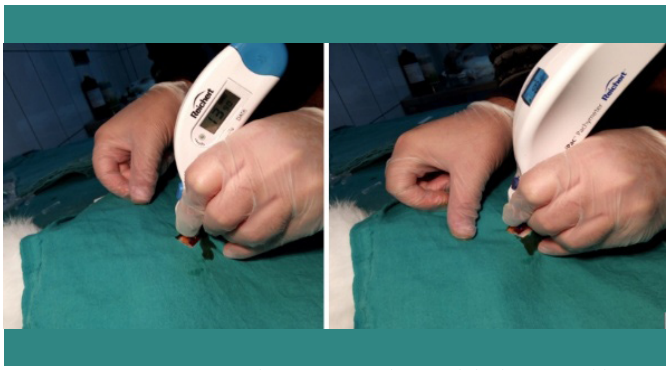

Figure 2. Measuring intraocular pressure and corneal thickness in rabbits

Table 1. Experimental protocol

Groups	Day 0	Day 7	Day 30
Control 1 (n: 5)	IV-BSS	Sample collection	X
Control 2 (n: 5)	IV-BSS	X	Sample collection
Group 1a (n: 8)	IV-0.1 N	Sample collection	X
Group 1b (n: 8)	IV-0.1 N	X	Sample collection
Group 2a (n: 8)	IV-0.05 N	Sample collection	X
Group 2b (n: 8)	IV-0.05 N	X	Sample collection

IV: Intravitreal injection, BSS: Balanced salt solution, N: Nepafenac

Histopathological Examination

At the end of the study period, the animals were sacrificed under deep anesthesia, and the globes were enucleated and fixed in 10% formalin solution. Then, standard histological tissue processing procedures were applied, and paraffin blocks were prepared. 4-5 µm thick sections obtained from the retinal tissue were stained with hematoxylin-eosin (H&E). Sections were evaluated under a light microscope for the integrity of retinal layers, cellular structure, and possible degenerative changes. Histopathological evaluations and terminal deoxynucleotidyl transferase-mediated dUTP nick end labelling (TUNEL) staining analyses were performed by a masked/blinded pathologist who was unaware of which group the samples belonged to.

TUNEL (Terminal Deoxynucleotidyl Transferase-Mediated dUTP Nick End Labeling) Analysis

The TUNEL method is a technique used to detect apoptotic cell death in tissues. This method shows nuclear DNA fragmentation by labeling the 3'-hydroxyl ends of breaks in the DNA strand during apoptosis. In our study, a commercially available TUNEL kit was used to identify apoptotic cells, in accordance with the manufacturer's recommendations. After staining, TUNEL-positive cells were evaluated under a light microscope, counted along the retinal layers, and the Apoptotic Index was calculated and compared between groups.

Statistical Analysis

All data analyses were performed using the Statistical Package for the Social Sciences (SPSS) version 20.0 for Windows (SPSS

Inc., Chicago, IL, USA). Since the parametric assumptions were not met, nonparametric tests were used. Comparisons among the three groups at each time point were performed using the Kruskal-Wallis test. Within-group comparisons across the three time points were performed using the Friedman test. A p-value of <0.05 was considered statistically significant.

RESULTS

Clinical Examination Findings

Intraocular pressure (IOP) and central corneal thickness (CCT) measurements obtained before injection and at 1 week and 1 month after injection did not differ significantly among the control, low-dose nepafenac, and high-dose nepafenac groups at any time point (p>0.05; Table 2). Similarly, no statistically significant changes in IOP or CCT were observed over time within any of the three groups (p>0.05).

TUNEL (Terminal Deoxynucleotidyl Transferase-mediated dUTP nick end labelling) Method

In the examinations performed with the TUNEL staining technique, TUNEL staining percentages (Apoptotic Index) were determined (Figure 5). Apoptosis indices are values obtained by counting 100 cells in 3 different areas where staining was observed; dividing the total number of positive cells by the total number of cells and expressing them as percentages. TUNEL staining percentages obtained before injection and at 1 week and 1 month after injection did not differ significantly among the control, low-dose nepafenac, and high-dose nepafenac groups at any time point (p>0.05; Table 3). Similarly, no statistically significant changes in TUNEL staining percentages were observed over time within any of the three groups (p>0.05).

Table 2. Comparison of intraocular pressure and central corneal thickness among the three groups at different time points

Parameter	Time point	Control	Group 1	Group 2	p-value
IOP (mmHg)	Pre-injection	11.40±2.01	12.13±1.92	12.63± 2.21	0.636
	1 week	10.00±2.54	10.20±2.30	10.94±2.48	0.496
	1 month	12.00±0.70	10.57±1.27	11.38±1.68	0.554
CCT (µm)	Pre-injection	401.60±24.07	373.73±20.96	371.25±23.97	0.316
	1 week	395.30±20.62	373.07±17.49	375.69±20.71	0.481
	1 month	397.40±4.93	369.43±19.10	383.75±20.14	0.596

Values are presented as mean±standard deviation. p-values represent comparisons among the three groups at each time point and were calculated using the Kruskal-Wallis test. IOP: Intraocular pressure, CCT: Central corneal thickness

Transient lens opacities were observed in 6 eyes (4 in the high-dose group and 2 in the low-dose group) at the 1-week follow-up, and all opacities completely resolved by the 1-month follow-up (Figure 3).

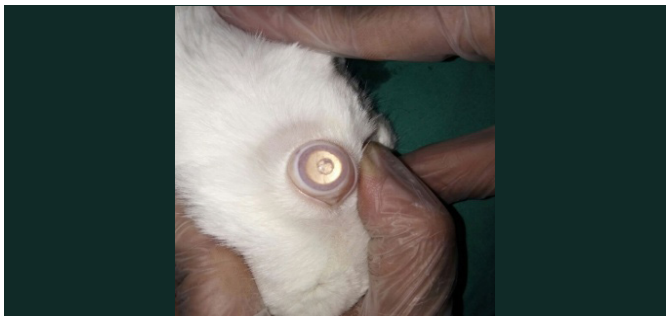

Figure 3. Eye showing cataract after injection

Histopathological Findings

Histopathological evaluations of biopsy sections from both the control and drug groups at 1 week and 1 month under light microscopy revealed no pathological findings at the retinal level (Figure 4).

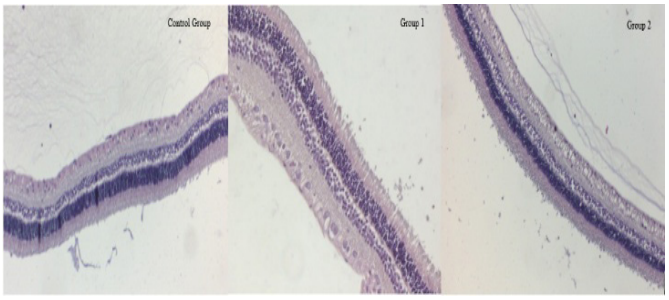

Figure 4. Hematoxylin/eosin staining patterns of all groups at 1 month

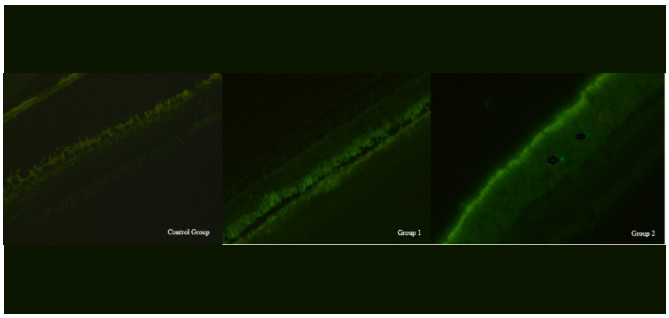

Figure 5. TUNEL staining patterns of all groups at 1 month (→apoptotic cells are observed)

TUNEL: Terminal deoxynucleotidyl transferase-mediated dUTP nick end labeling

Table 3. TUNEL staining percentages of the working eyes of all groups

Parameter	Time point	Control	Group 1	Group 2	p-value
TUNEL	1 week%	1.60±2.19	0.75±1.75	1.00±1.69	0.738
	1 month%	1.60±2.07	2.14±1.95	1.38±1.68	0.598

*TUNEL: Terminal deoxynucleotidyl transferase-mediated dUTP nick end labeling

DISCUSSION

In the present study, the potential retinal toxicity of intravitreal nepafenac was evaluated using clinical, histopathological, and apoptotic parameters in a rabbit model. Our findings demonstrate that intravitreal nepafenac, at both tested doses, did not induce significant structural damage or increased apoptotic cell death in the retina in the short to medium term.

In recent years, advances in the understanding of retinal inflammation have highlighted the critical role of prostaglandin-mediated pathways not only in cystoid macular edema but also in diabetic macular edema and

retinal vascular diseases.[17-19] These insights suggest that anti-inflammatory therapies should be considered not only as symptomatic treatments but also as potential pathogenetic interventions. However, the well-known adverse effects of intravitreal corticosteroids, including cataract formation and elevated intraocular pressure, necessitate the investigation of safer alternative agents.

Although anti-VEGF therapies remain the cornerstone of treatment for retinal vascular diseases, recent studies have demonstrated that inflammation may contribute significantly to suboptimal responses in a subset of patients.[20] The adjunctive role of anti-inflammatory agents is therefore increasingly emphasized, particularly in resistant or partially responsive macular edema.[21] In this context, identifying safe intravitreal anti-inflammatory alternatives to corticosteroids is of growing clinical importance. The findings of the present study contribute to this need by demonstrating a favorable retinal safety profile for intravitreal nepafenac.

Experimental studies investigating the intravitreal use of NSAIDs remain limited; however, available data suggest that agents such as ketorolac, diclofenac, bromfenac, and aspirin do not produce significant retinal toxicity.[22-26] These findings indicate that NSAIDs may offer a safer side-effect profile compared to corticosteroids. Nepafenac, in particular, is a prodrug that is rapidly converted to its active metabolite, amfenac, and has been shown to exhibit low cytotoxicity, making it a promising candidate for intravitreal administration.[27,28]

The study by Afrashi et al.[29] represents one of the few investigations specifically evaluating intravitreal nepafenac in a rabbit model. In that study, no significant retinal toxicity was observed based on clinical examination, electroretinography, and histopathological assessment. Our findings are consistent with these results and further extend them by incorporating evaluation of apoptotic cell death using the TUNEL method. While previous studies primarily focused on structural and functional outcomes, our study provides additional insight at the cellular level. By demonstrating the absence of increased apoptosis alongside preserved retinal architecture, our results offer a more comprehensive assessment of retinal safety. In this respect, our study not only confirms but also expands upon previous findings by providing a more detailed evaluation of potential subclinical toxicity.

Recent retinal toxicity studies emphasize that preservation of histopathological integrity alone may not be sufficient to exclude toxicity, and that evaluation of apoptotic processes is essential for detecting subclinical damage. TUNEL analysis has therefore emerged as a valuable tool in this context.[30,31] The combined use of histopathological and apoptotic assessments in our study represents a strength and aligns with current approaches to retinal toxicity evaluation.

Another important aspect of our study is the evaluation of both dose-dependent and time-dependent effects. Many previous studies have been limited to a single dose or time point, whereas our design included multiple doses and two distinct evaluation periods. This approach allows for a more comprehensive assessment of both early and subacute toxic effects.

In our study, mild and transient lens opacities were observed in a small number of eyes during the early postoperative period. These findings are consistent with previous reports on intravitreal NSAID use. The earlier onset and higher frequency of lens opacities in the high-dose group suggest a possible dose-related pharmacokinetic effect. Although these opacities resolved completely by the first-month follow-up, the potential cumulative effects of repeated intravitreal nepafenac injections remain unclear and warrant further investigation.

Limitations

This study has several limitations. First, the experimental model was performed in healthy rabbit eyes; therefore, the retinal safety of intravitreal nepafenac was not evaluated under pathological conditions such as diabetic retinopathy, retinal vascular occlusion, or uveitis. Second, only a single intravitreal injection was administered, and the potential cumulative effects of repeated dosing were not investigated. Third, functional retinal assessments, such as electroretinography, were not performed. Finally, although retinal histology and apoptosis were comprehensively evaluated, possible effects on other ocular tissues, including the cornea, iris, and ciliary body, were beyond the scope of the present study. Forth, an a priori sample size calculation was not performed, and the relatively limited sample size may have reduced the statistical power to detect small or subtle differences. Therefore, the absence of statistically significant differences should be interpreted cautiously and does not necessarily exclude the possibility of small biological effects. Future studies incorporating disease models, repeated injections, functional retinal testing, and comprehensive ocular toxicity assessments are warranted to further establish the safety profile of intravitreal nepafenac.

CONCLUSION

Intravitreal administration of nepafenac did not result in significant retinal toxicity with respect to histological integrity or apoptotic activity in this experimental rabbit model. These findings suggest that nepafenac may represent a promising intravitreal anti-inflammatory agent with a favorable retinal safety profile. Nevertheless, additional experimental studies involving repeated dosing, disease models, functional retinal assessments, and long-term follow-up are required before its potential clinical application can be considered.

ETHICAL DECLARATIONS

Ethics Committee Approval

This study was approved by the Kırıkkale University Experimental Animal Ethics Committee (Date: 25.02.2016, Decision No: 16/35).

Informed Consent

This study was conducted using experimental animals; as it did not involve human participants, written informed consent was not obtained.

Peer Review Process

This manuscript was subject to external peer review.

Conflict of Interest

The authors declare no conflicts of interest related to this study.

Financial Disclosure

This study was supported by the Kırıkkale University Scientific Research Projects Unit (BAP) (Project No: 2016/130). Funding

covered the costs of purchasing and caring for experimental animals and TUNEL assay kits.

Author Contributions

Concept: YÖ, TO, NÖ, ZO, RO; Design: YÖ, TO, NÖ, ZO, RO; Control: YÖ, TO, NÖ, ZO, RO; Resources: YÖ, TO, NÖ, ZO, RO; Materials: YÖ, TO, NÖ, ZO, RO; Data Collection and/or Processing YÖ, TO, NÖ, ZO, RO; Analysis and/or Interpretation YÖ, TO, NÖ, ZO, RO; Literature Review: YÖ, TO, NÖ, ZO, RO; Writing the Article: YÖ, TO, NÖ, ZO, RO; Critical Review: YÖ, TO, NÖ, ZO, RO.

REFERENCES

1. Fong DS, Ferris FL 3rd, Davis MD, Chew EY. Causes of severe visual loss in the early treatment diabetic retinopathy study: ETDRS report no. 24. *Am J Ophthalmol.* 1999;127(2):137-141. doi:10.1016/S0002-9394(98)00309-2
2. Gutman FA, Zegarra H. Macular edema secondary to occlusion of the retinal veins. *Surv Ophthalmol.* 1984;28(suppl):462-470. doi:10.1016/0039-6257(84)90228-5
3. Gass JD, Norton EW. Follow-up study of cystoid macular edema following cataract extraction. *Trans Am Acad Ophthalmol Otolaryngol.* 1969;73(4):665-682.
4. Hitchings RA, Chisholm IH. Incidence of aphakic macular oedema: a prospective study. *Br J Ophthalmol.* 1975;59(8):444-450. doi:10.1136/bjo.59.8.444
5. Jonas JB, Kreissig I, Degenring R. Intravitreal triamcinolone acetonide for treatment of intraocular proliferative, exudative, and neovascular diseases. *Prog Retin Eye Res.* 2005;24(5):587-611. doi:10.1016/j.preteyeres.2005.01.004
6. Kogure A, Ohkoshi K, Kogure S, Yamaguchi T, Kishi S. Efficacy and retention times of intravitreal triamcinolone acetonide for macular edema. *Jpn J Ophthalmol.* 2008;52(2):122-126. doi:10.1007/S10384-007-0513-7
7. Haller JA, Bandello F, Belfort R Jr, et al. Randomized, sham-controlled trial of dexamethasone intravitreal implant in patients with macular edema due to retinal vein occlusion. *Ophthalmology.* 2010;117(6):1134-1146.e3. doi:10.1016/j.ophtha.2010.03.032
8. Goñi FJ, Stalmans I, Denis P, et al. Elevated intraocular pressure after intravitreal steroid injection in diabetic macular edema: monitoring and management. *Ophthalmol Ther.* 2016;5(1):47-61. doi:10.1007/S40123-016-0052-8
9. Vane JR, Botting RM. Mechanism of action of nonsteroidal anti-inflammatory drugs. *Am J Med.* 1998;104(3A):2S-22S. doi:10.1016/S0002-9343(97)00203-9
10. Wielders LH, Lambermont VA, Schouten JS, et al. Prevention of cystoid macular edema after cataract surgery in nondiabetic and diabetic patients: a systematic review and meta-analysis. *Am J Ophthalmol.* 2015;160(5):968-981.e33. doi:10.1016/j.ajo.2015.07.032
11. Semeraro F, Russo A, Gambicorti E, et al. Efficacy and vitreous levels of topical NSAIDs. *Expert Opin Drug Deliv.* 2015;12(11):1767-1782. doi:10.1517/17425247.2015.1068756
12. Lane SS. Nepafenac: a unique nonsteroidal prodrug. *Int Ophthalmol Clin.* 2006;46(4):13-20. doi:10.1097/01.IIO.0000212129.53019.49
13. Singh R, Alpern L, Jaffe GJ, et al. Evaluation of nepafenac in prevention of macular edema following cataract surgery in patients with diabetic retinopathy. *Clin Ophthalmol.* 2012;6:1259-1269. doi:10.2147/OPTH.S31902
14. Gamache DA, Graff G, Brady MT, Spellman JM, Yanni JM. Nepafenac, a unique nonsteroidal prodrug with potential utility in the treatment of trauma-induced ocular inflammation. I. assessment of anti-inflammatory efficacy. *Inflammation.* 2000;24(4):357-370. doi:10.1023/A:1007049015148
15. Hariprasad SM, Callanan D, Gainey S, He YG, Warren K. Cystoid and diabetic macular edema treated with nepafenac 0.1%. *J Ocul Pharmacol Ther.* 2007;23(6):585-590. doi:10.1089/jop.2007.0062
16. Alkin Z, Osmanbasoglu OA, Ozkaya A, Karatas G, Yazici AT. Topical nepafenac in treatment of acute central serous chorioretinopathy. *Med Hypothesis Discov Innov Ophthalmol.* 2013;2(4):96-101.
17. Gurung RL, FitzGerald LM, Liu E, et al. Predictive factors for treatment outcomes with intravitreal anti-vascular endothelial growth factor injections in diabetic macular edema in clinical practice. *Int J Retina Vitreous.* 2023;9(1):23. doi:10.1186/S40942-023-00453-0
18. Ng DSC, Ruamviboonsuk P, Apte RS, et al. International consensuses and controversies on causes, diagnosis and management of diabetic macular edema. *Prog Retin Eye Res.* 2025;109:101406. doi:10.1016/j.preteyeres.2025.101406
19. Srejovic JV, Muric MD, Jakovljevic VL, et al. Molecular and cellular mechanisms involved in the pathophysiology of retinal vascular disease: interplay between inflammation and oxidative stress. *Int J Mol Sci.* 2024;25(21):11850. doi:10.3390/ijms252111850
20. Walsh JO, Gallemore RP. Anti-VEGF-resistant retinal diseases: a review of the latest treatment options. *Cells.* 2021;10(5):1049. doi:10.3390/cells10051049
21. Hatamnejad A, Orr S, Dadak R, et al. Anti-VEGF and steroid combination therapy relative to anti-VEGF monotherapy for the treatment of refractory diabetic macular edema: a systematic review of efficacy and meta-analysis of safety. *Acta Ophthalmol.* 2024;102(3):e204-e214. doi:10.1111/aos.15724
22. Margalit E, Kugler LJ, Brumm MV, et al. The safety of intraocular ketorolac in rabbits. *Invest Ophthalmol Vis Sci.* 2006;47(5):2093-2099. doi:10.1167/iovs.05-0764
23. Komarowska I, Heilweil G, Rosenfeld PJ, Perlman I, Loewenstein A. Retinal toxicity of commercially available intravitreal ketorolac in albino rabbits. *Retina.* 2009;29(1):98-105. doi:10.1097/IAE.0b013e31817d8c09
24. Kim SJ, Adams NA, Toma HS, et al. Safety of intravitreal ketorolac and diclofenac: an electroretinographic and histopathologic study. *Retina.* 2008;28(4):595-605. doi:10.1097/IAE.0b013e31815e98a5
25. Dogan C, Yetik H, Arslan OS, et al. The safety of intraocular usage of aspirin. *Cutan Ocul Toxicol.* 2019;38(2):201-205. doi:10.1080/15569527.2019.1575391
26. Sánchez-Santos I, García-Sánchez GA, Gonzalez-Salinas R, et al. Intravitreal bromfenac liposomal suspension (100 µg/0.1 ml): a safety study in rabbit eyes. *Exp Eye Res.* 2020;194:108020. doi:10.1016/j.exer.2020.108020
27. Ke TL, Graff G, Spellman JM, Yanni JM. Nepafenac, a unique nonsteroidal prodrug with potential utility in the treatment of trauma-induced ocular inflammation. II. in vitro bioactivation and permeation of external ocular barriers. *Inflammation.* 2000;24(4):371-384. doi:10.1023/A:1007001131987
28. Lindstrom R, Kim T. Ocular permeation and inhibition of retinal inflammation: an examination of data and expert opinion on the clinical utility of nepafenac. *Curr Med Res Opin.* 2006;22(2):397-404. doi:10.1185/030079906X89775
29. Afrashi F, Hashas AS, Shahbazov C, et al. Reliability of intravitreal nepafenac in rabbits. *J Ocul Pharmacol Ther.* 2015;31(1):43-50. doi:10.1089/jop.2014.0053
30. Lin H, Yue Y, Maidana DE, et al. Drug delivery nanoparticles: toxicity comparison in retinal pigment epithelium and retinal vascular endothelial cells. *Semin Ophthalmol.* 2016;31(1-2):1-9. doi:10.3109/08820538.2015.1114865
31. Zhang Z, Zhao L, Ma Y, et al. Mechanistic study of silica nanoparticles on the size-dependent retinal toxicity in vitro and in vivo. *J Nanobiotechnol.* 2022;20(1):146. doi:10.1186/S12951-022-01326-8

Archives of
Ophthalmological Research

Original Article

DOI: 10.51271/AOR-0056

Multimodal retinal imaging-based assessment of large language models for the differential diagnosis of retinal vascular occlusion

Memduh Kurt, Ayna Sariyeva Ismayilov*, Mahmut Oğuz Ulusoy

Department of Ophthalmology, University of Health Sciences Bursa Yüksek İhtisas Training and Research Hospital, Bursa, Turkiye

Cite this article: Kurt M, Sariyeva Ismayilov A, Ulusoy MO. Multimodal retinal imaging-based assessment of large language models for the differential diagnosis of retinal vascular occlusion. *Arch Ophthalmol Res.* 2026;3(3):52-56. doi:10.51271/AOR-0056

Received: 29/06/2026 ◆ **Accepted:** 21/09/2026 ◆ **Published:** 24/09/2026

ABSTRACT

Aims: To compare the diagnostic and treatment recommendation performance of three large language models (LLMs)-ChatGPT-4o, Gemini, and Microsoft Copilot-in the differential diagnosis of retinal vascular occlusions using multimodal retinal imaging.

Methods: This observational study included 75 patients, comprising 50 retinal vein occlusion (RVO; 25 branch and 25 central) and 25 retinal artery occlusion (RAO; 6 branch and 19 central) cases. Each LLM independently evaluated three imaging datasets: (1) color fundus photographs, (2) fundus photographs combined with optical coherence tomography (OCT), and (3) fundus photographs combined with OCT and fundus fluorescein angiography (FFA). A standardized prompt was used for all analyses. Diagnostic accuracy and treatment recommendation accuracy were compared among the models using Cochran's Q and post-hoc McNemar tests.

Results: Significant differences in diagnostic accuracy were observed among the three models under all imaging conditions (all $p<0.001$). Using fundus photographs alone, diagnostic accuracy was 21.3% for ChatGPT-4o, 12.0% for Gemini, and 1.3% for Copilot. After adding OCT images, ChatGPT-4o and Gemini each achieved an accuracy of 21.3%, whereas Copilot remained at 1.3%. With multimodal imaging (fundus photographs+OCT+FFA), diagnostic accuracy increased to 28.0% for ChatGPT-4o and 37.3% for Gemini, while Copilot again remained unchanged at 1.3%. Pairwise comparisons demonstrated no significant difference between ChatGPT-4o and Gemini across imaging conditions, whereas both significantly outperformed Copilot. For treatment recommendations, Gemini achieved the highest accuracy (57.3%), followed by ChatGPT-4o (26.7%) and Copilot (10.7%) ($p<0.001$). Gemini performed significantly better than both ChatGPT-4o and Copilot, and ChatGPT-4o also outperformed Copilot.

Conclusion: Although multimodal retinal imaging improved the diagnostic performance of current LLMs, their overall diagnostic accuracy remained inadequate for independent clinical use in retinal vascular occlusions. Gemini demonstrated the greatest benefit from multimodal image integration and provided the most accurate treatment recommendations. These findings suggest that current LLMs should be regarded as supportive clinical tools rather than autonomous diagnostic systems, while future multimodal Artificial Intelligence models trained on ophthalmology-specific datasets may achieve substantially improved performance.

Keywords: Retinal vascular occlusion, retinal vein occlusion, retinal artery occlusion, large language models, multimodal imaging, Artificial Intelligence

INTRODUCTION

In recent years, Artificial Intelligence (AI) technologies have become an integral component of daily life and an essential tool for addressing complex problems. This technological transformation has created new opportunities in medicine and health sciences. In the field of ophthalmology, in particular, the ability of AI algorithms to analyze data derived from imaging modalities and detect pathological findings offers considerable potential for the development of clinical decision-support systems.

According to the International Diabetes Federation (IDF), the global prevalence of diabetes mellitus is expected to reach 700 million by 2045.[1] Therefore, image-based autonomous diagnostic systems in the field of ophthalmology have predominantly focused on diabetic retinopathy. A Google DeepMind deep learning algorithm trained on diabetic retinopathy datasets demonstrated high sensitivity, specificity, and accuracy in detecting diabetic retinopathy using color fundus photographs.[2] Considering the anticipated decline in the number of physicians per patient, the use of autonomous

***Corresponding Author:** Ayna Sariyeva Ismayilov, sariyevaayna@hotmail.com

systems is expected to become increasingly widespread. Moreover, several studies have suggested that AI-assisted screening may be more cost-effective than conventional screening performed by ophthalmologists.[3]

In addition, algorithms capable of classifying age-related macular degeneration (AMD) according to the AREDS severity scale are currently available.[4] These studies indicate that AI can achieve success rates approaching 99% through image-based deep learning. However, without requiring task-specific deep learning training, readily accessible large language models (LLMs), such as Chat Generative Pre-trained Transformer-4 (ChatGPT-4o; OpenAI), Google Gemini (Alphabet Inc.), and Microsoft Copilot (Microsoft Corporation), are increasingly used by both patients and physicians in diagnostic and therapeutic processes in healthcare. Today, these systems play a critical role not only in the detection of various fundus pathologies but also in the screening and early diagnosis of systemic diseases through retinal assessment.[5] Researchers in Singapore[6,7] and South Korea[8,9] have developed deep learning systems (DLSs) implemented in public healthcare settings to detect referable eye diseases, including glaucoma, AMD, and diabetic retinopathy, with high accuracy.

Although the increasing use of LLMs in healthcare presents both advantages and limitations for physicians and patients, these tools may offer substantial potential when applied with appropriate clinical awareness and consideration of potential biases. While AI has demonstrated competence in information delivery, its reliability and diagnostic accuracy in medical practice remain to be fully established through comprehensive academic research. Therefore, this study aims to assess the performance and clinical reliability of current LLM platforms in the interpretation of imaging findings associated with retinal vascular diseases.

METHODS

Ethics

The study protocol was formally approved by the University of Health Sciences Bursa Yüksek İhtisas Training and Research Hospital Medical Sciences Ethics Committee (Date: 22.04.2026, Decision No: 2024-TBEK 2026/04-10) in accordance with the Declaration of Helsinki.

Study Design

A total of 75 patients were included in the study, comprising 50 patients diagnosed with retinal vein occlusion (RVO; 25 central and 25 branch retinal vein occlusions) and 25 patients diagnosed with retinal artery occlusion (RAO; 19 central and 6 branch retinal artery occlusions).

The mean duration of symptoms before hospital presentation was 4.02±2.64 days (range, 0-8 days) in the RAO group and 15.04±3.14 days (range, 1-21 days) in the RVO group. Fundus photography, OCT, and FFA were performed on the day of presentation, and these examinations represented the patients' initial imaging assessments. Patients with chronic or diagnostically ambiguous retinal vascular occlusions were excluded. All patients were evaluated and managed by experienced retina specialists independently of the LLM-generated responses. The LLMs were subsequently provided with the same initial imaging data used by the retina specialists for diagnosis.

The diagnostic performances of large language models (LLMs) were evaluated using three different datasets: (1) fundus photographs obtained at a 50-degree angle, including the optic disc, macula, and major vascular arcades; (2) a combination of fundus photographs and optical coherence tomography (OCT) images; and (3) a triple-modality combination consisting of fundus photographs, OCT images, and fundus fluorescein angiography (FFA) images. The analyses were performed independently by each model using ChatGPT-4o, Gemini, and Copilot software.

The fundus photographs (Topcon TRC-50DX, Japan), OCT images (RTVue XR Avanti, Optovue, Inc., Fremont, CA, USA), and FFA images (Topcon TRC-50DX, Japan) used in the study were retrospectively obtained from the archive of the Depatment of Retina of Bursa Yüksek İhtisas Training and Research Hospital. A multimodal approach was adopted to ensure that the responses generated by the AI models were based directly on visual data. The data input process was carried out between December 27, 2025, and January 4, 2026. Each model was queried using a standardized prompt: "I will present you with an image; can you diagnose the disease?"

The models' abilities to interpret pathological findings in the images and their diagnostic accuracy rates were recorded. To minimize potential memory bias and prevent the models from learning from previous queries, each session was terminated after every analysis, and a new chat was initiated. Fundus photographs, OCT images, and FFA combinations were queried separately in different chat windows, and the accuracy of the findings and diagnoses was recorded prospectively. As examinations from 75 patients were presented to each AI application in three different combinations, a total of 675 queries were analyzed within the scope of the study.

Statistical Analysis

All data analyses were performed using IBM SPSS Statistics version 23.0. The normality of continuous variables was assessed using the Kolmogorov-Smirnov test. Continuous variables that did not show a normal distribution were presented as median minimum-maximum values, while categorical variables were expressed as numbers and percentages.

The responses of the AI models regarding diagnosis and treatment recommendations were coded as "correct" or "incorrect." Since the same 75 cases were evaluated by all models, Cochran's Q test was used to compare the accuracy rates of the three models (Figure 1). When a significant difference was detected in the overall comparison, pairwise post-hoc comparisons were performed using McNemar's test.

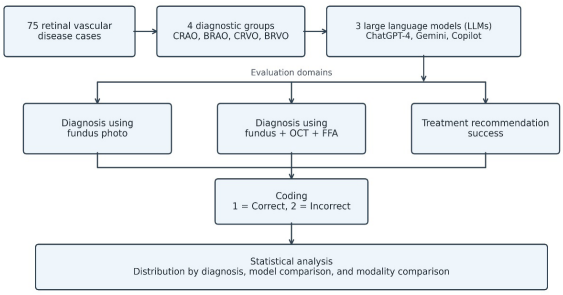

Figure 1. Study flow diagram

CRAO: Central retinal artery occlusion, BRAO: Branch retinal artery occlusion, CRVO: Central retinal vein occlusion, BRVO: Branch retinal vein occlusion, ChatGPT: Chat Generative Pre-trained Transformer, OCT: Optical coherence tomography, FFA: Fundus fluorescein angiography

RESULTS

A total of 50 patients with retinal vein occlusion, including 25 with branch retinal vein occlusion (BRVO) and 25 with central retinal vein occlusion (CRVO), and 25 patients with retinal artery occlusion, including 6 with branch retinal artery occlusion (BRAO) and 19 with central retinal artery occlusion (CRAO), were included in the evaluation. As the data of 75 patients were presented to each AI application in three different combinations, a total of 675 queries/prompts were performed.

In the RAO group, there were 7 female (28%) and 18 male (72%), whereas the RVO group included 23 female (46%) and 27 male (54%) (p=0.105). The mean age was 62.52±11.95 years in the RAO group (range: 40-86) and 64.62±11.52 years in the RVO group (range: 43-75). No statistically significant difference was observed between the groups in terms of age (p=0.465) (Table 1).

Table 1. Distribution of age and gender according to diagnostic groups

Diagnostic group	n	Age, median (min-max)	Female n (%)	Male n (%)
CRAO	19	64 (19-76)	4 (21.1)	15 (78.9)
BRAO	6	63.5 (55-76)	3 (50.0)	3 (50.0)
CRVO	25	69 (51-92)	11 (44.0)	14 (56.0)
BRVO	25	57 (40-85)	12 (48.0)	13 (52.0)
Total	75	65 (19-92)	30 (40.0)	45 (60.0)

Age data are presented as median (minimum-maximum), and gender data are presented as n (%). Min: Minimum, Max: Maximum, CRAO: Central retinal artery occlusion, BRAO: Branch retinal artery occlusion, CRVO: Central retinal vein occlusion, BRVO: Branch retinal vein occlusion

When fundus photographs alone were evaluated, a significant difference was observed among the three models (Cochran's Q, p<0.001). ChatGPT-4o demonstrated the highest diagnostic accuracy, followed by Gemini, whereas Copilot showed the lowest performance. Pairwise comparisons revealed no significant difference between ChatGPT-4o and Gemini, while both models significantly outperformed Copilot (Table 2).

The addition of OCT did not improve the diagnostic accuracy of ChatGPT-4o or Gemini compared with fundus photography alone. Nevertheless, a significant difference remained among the three models, with ChatGPT-4o and Gemini performing significantly better than Copilot. There was no significant difference between ChatGPT-4o and Gemini (Table 2).

With the addition of FFA to fundus photography and OCT, diagnostic performance increased for both ChatGPT-4o and Gemini, with Gemini achieving the highest overall diagnostic accuracy. However, the difference between ChatGPT-4o and Gemini remained statistically nonsignificant. Both models continued to significantly outperform Copilot, whose diagnostic accuracy remained unchanged across all imaging conditions (Table 2).

For treatment recommendations, a significant difference was observed among the three models (p<0.001). Gemini demonstrated the highest accuracy and significantly outperformed both ChatGPT-4o and Copilot. ChatGPT-4o also performed significantly better than Copilot (Table 2; Figure 2).

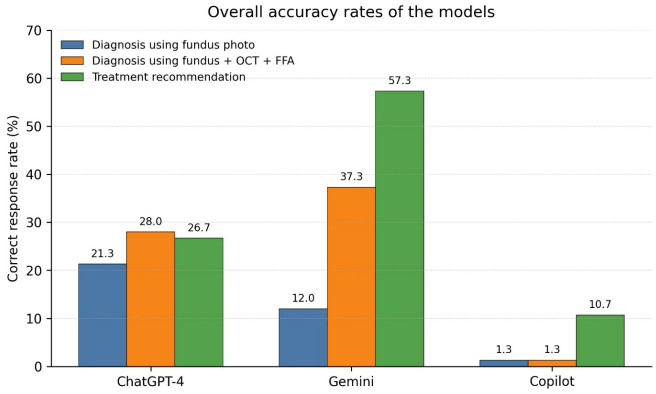

Figure 2. Overall accuracy rates of the models

OCT: Optical coherence tomography, FFA: Fundus fluorescein angiography, ChatGPT: Chat Generative Pre-trained Transformer

Detailed diagnostic and treatment recommendation accuracy rates and pairwise comparisons are presented in Table 2.

DISCUSSION

CRAO is estimated to occur at an incidence of 1-2 cases per 100,000 individuals per year.[10] The importance of early diagnosis is not limited to the intended visual prognosis; it is also critical in terms of the patient's morbidity and mortality risk. The interval between symptom onset and presentation to

Table 2. Overall model performance according to assessment domains

Assessment domain	Model	Correct n (%)	Overall p (Cochran's Q)	ChatGPT-4o vs Gemini	ChatGPT-4o vs Copilot	Gemini vs Copilot
Diagnosis using fundus photographs	ChatGPT-4o	16 (21.3)	<0.001	0.143	<0.001	0.021
	Gemini	9 (12.0)				
	Copilot	1 (1.3)				
Diagnosis using fundus photographs+OCT	ChatGPT-4o	16 (21.3)	<0.001	1.000	<0.001	<0.001
	Gemini	16 (21.3)				
	Copilot	1 (1.3)				
Diagnosis using fundus photographs+OCT+FFA	ChatGPT-4o	21 (28.0)	<0.001	0.248	<0.001	<0.001
	Gemini	28 (37.3)				
	Copilot	1 (1.3)				
Treatment recommendation	ChatGPT-4o	20 (26.7)	<0.001	<0.001	0.013	<0.001
	Gemini	43 (57.3)				
	Copilot	8 (10.7)				

Data are presented as the number and percentage of correct responses. Overall comparisons were performed using Cochran's Q test. Pairwise pos- hoc comparisons were performed using McNemar's test. ChatGPT: Chat Generative Pre-trained Transformer, OCT: Optical coherence tomography, FFA: Fundus fluorescein angiography

an ophthalmologist is of crucial importance. Unfortunately, in some clinical scenarios, this interval may extend to several days. With the increasing use of AI-based fundus image screening tools, this delay is expected to decrease.

RVO is the second most common retinal vascular disease leading to visual impairment and blindness after diabetic retinopathy. In 2015, the global prevalence of RVO, BRVO, and CRVO among individuals aged 30-89 years was reported as 0.77%, 0.64%, and 0.13%, respectively, corresponding to approximately 28.06 million, 23.38 million, and 4.67 million affected individuals worldwide.[11] Early diagnosis and timely treatment contribute positively to final visual acuity outcomes.

Previous studies have also demonstrated that RVO is associated with cardiovascular risk factors such as arterial hypertension, family history of stroke, and atrial fibrillation.[12,13] Therefore, early diagnosis of retinal vascular diseases may provide important benefits in terms of reducing morbidity and mortality. Through early detection, underlying systemic conditions such as hypertension, diabetes mellitus, or occult thrombophilia/hypercoagulability in younger patients may be identified at an earlier stage, thereby potentially reducing the risk of systemic thromboembolic events.

Limitations

This study comparatively demonstrated the clinical capabilities of current LLMs in the diagnosis and treatment planning of retinal vascular diseases. Our findings reflect the sensitivity of AI models to multimodal data input, as well as their current limitations within clinical decision-support mechanisms.

An important distinction should be made between our findings and those reported by Gulshan et al.,[2] who developed and validated a deep convolutional neural network specifically designed for the detection of diabetic retinopathy and diabetic macular edema from retinal fundus photographs. Their algorithm was trained on a large, task-specific dataset of 128,175 retinal images and achieved very high diagnostic performance, with area under the receiver operating characteristic curve values of approximately 0.99 in two independent validation datasets. In contrast, the models evaluated in our study were general-purpose LLMs that were not specifically developed or fine-tuned for the diagnosis of retinal vascular occlusions. Therefore, the substantially lower diagnostic performance observed in our study should not be interpreted as evidence that AI is inherently inadequate for ophthalmic image interpretation. Rather, the difference likely reflects the fundamentally different design and training objectives of these systems. Task-specific deep-learning algorithms are optimized for a predefined ophthalmic classification task using large, carefully annotated image datasets, whereas general-purpose LLMs are designed to perform a broad range of language and multimodal tasks and may lack disease-specific optimization. Furthermore, Gulshan et al.[2] evaluated a well-defined diabetic retinopathy detection task using standardized fundus photographs, whereas our study addressed the more challenging differential diagnosis of retinal vascular occlusions, including CRAO, CRVO, and BRVO, and further examined whether incorporating complementary OCT and FFA information could improve performance. Thus, our findings highlight both the potential and the current limitations of general-purpose LLMs in ophthalmic image interpretation and suggest that their performance should be interpreted differently from that of task-specific deep-learning systems.

Overall, all three models demonstrated limited diagnostic performance when interpreting retinal vascular occlusions from fundus photographs alone, with ChatGPT-4o showing relatively better performance than Gemini and Copilot. The addition of OCT did not substantially improve ChatGPT's overall diagnostic performance, whereas Gemini showed a more favorable ability to recognize CRAO and cherry-red spot findings when OCT information was incorporated. The most notable improvement was observed with the combined presentation of fundus photography, OCT, and FFA, particularly for Gemini, suggesting that access to complementary multimodal imaging information may enhance the interpretation of retinal vascular abnormalities by some general-purpose LLMs. In contrast, Copilot showed consistently poor performance across all imaging configurations, indicating that the addition of multimodal information alone was insufficient to improve its image-based diagnostic capability. Treatment recommendations followed a similar pattern, with Gemini demonstrating greater consistency with current clinical management principles than ChatGPT-4o and Copilot. Interestingly, Copilot occasionally provided appropriate treatment recommendations despite poor diagnostic performance, largely because it could recognize findings such as cystoid macular edema on OCT.

From a clinical perspective, our findings suggest that general-purpose LLMs currently have limited utility as standalone diagnostic tools for retinal vascular occlusions. Although the integration of multimodal imaging, particularly the combination of fundus photography, OCT, and FFA, improved diagnostic performance in some models, the maximum accuracy achieved remained insufficient to support independent clinical decision-making. Nevertheless, the observed improvement with multimodal information suggests that LLMs may have a potential role as supportive tools by integrating complementary imaging findings and assisting clinicians in generating differential diagnoses or management considerations. Importantly, such applications should be considered adjunctive rather than substitutive, and all diagnostic and treatment decisions should remain under the supervision of an ophthalmologist. To our knowledge, this is the first study to evaluate general-purpose LLMs in the multimodal interpretation of retinal vascular occlusions, including CRAO, CRVO, and BRVO, while also assessing their treatment recommendations. By evaluating different combinations of fundus photography, OCT, and FFA, our study provides preliminary evidence regarding both the potential and current limitations of general-purpose LLMs in this specific ophthalmic context.

CONCLUSION

To the best of our knowledge, this is the first study in the literature to compare the performance of current LLMs in the diagnosis and treatment recommendations of retinal vascular diseases using multimodal data. Our findings demonstrated that, despite the limitations of AI in single-image analysis, the integration of clinical imaging data, including fundus photography, OCT, and FFA, through a multimodal approach can significantly improve diagnostic performance. Despite their current limitations, these models hold potential as "clinical assistants," and further training with more specific

datasets may pave the way for a new era in the management of retinal diseases.

ETHICAL DECLARATIONS

Ethics Committee Approval

This study was approved by the University of Health Sciences Bursa Yüksek İhtisas Training and Research Hospital Medical Sciences Ethics Committee (Date: 22.04.2026, Decision No: 2024-TBEK 2026/04-10).

Informed Consent

Written informed consent was obtained from all individual participants prior to their inclusion in the study. Participants were fully informed about the study's aims, procedures, potential risks and benefits, and their rights-including the right to withdraw at any time without consequence. All participants voluntarily signed a written informed consent form.

Peer Review Process

This manuscript was subject to external peer review.

Conflict of Interest

The authors declare no conflicts of interest related to this study.

Financial Disclosure

The authors received no financial support for the conduct or publication of this research.

Author Contributions

Concept: MK, ASI, MOU; Design: MK, ASI, MOU; Control: MK, ASI, MOU; Resources: MK, ASI, MOU; Materials: MK, ASI, MOU; Data Collection and/or Processing: MK, ASI, MOU; Analysis and/or Interpretation: MK, ASI, MOU; Literature Review: MK, ASI, MOU; Writing the Article: MK, ASI, MOU; Critical Review: MK, ASI, MOU.

REFERENCES

1. Saeedi P, Petersohn I, Salpea P, et al. Global and regional diabetes prevalence estimates for 2019 and projections for 2030 and 2045: results from the International Diabetes Federation Diabetes Atlas, 9th edition. *Diabetes Res Clin Pract.* 2019;157:107843. doi:10.1016/j.diabres.2019.107843
2. Gulshan V, Peng L, Coram M, et al. Development and validation of a deep learning algorithm for detection of diabetic retinopathy in retinal fundus photographs. *JAMA.* 2016;316(22):2402-2410. doi:10.1001/jama.2016.17216
3. Huang XM, Yang BF, Zheng WL, et al. Cost-effectiveness of Artificial Intelligence screening for diabetic retinopathy in rural China. *BMC Health Serv Res.* 2022;22(1):260. doi:10.1186/s12913-022-07655-6
4. Peng Y, Dharssi S, Chen Q, et al. DeepSeeNet: A deep learning model for automated classification of patient-based age-related macular degeneration severity from color fundus photographs. *Ophthalmology.* 2019;126(4):565-575. doi:10.1016/j.ophtha.2018.11.015
5. Li Z, Wang L, Wu X, et al. Artificial Intelligence in ophthalmology: the path to the real-world clinic. *Cell Rep Med.* 2023;4(7):101095. doi:10.1016/j.xcrm.2023.101095
6. Ting DSW, Cheung CY, Lim G, et al. Development and validation of a deep learning system for diabetic retinopathy and related eye diseases using retinal images from multiethnic populations with diabetes. *JAMA.* 2017;318(22):2211-2223. doi:10.1001/jama.2017.18152
7. Wong DCS, Kiew G, Jeon S, Ting D. Singapore eye lesions analyzer (SELENA): the deep learning system for retinal diseases. In: Grzybowski A, editor. Artificial Intelligence in Ophthalmology. Cham: Springer; 2021:177-185. doi:10.1007/978-3-030-78601-4_13
8. Xie Y, Nguyen QD, Hamzah H, et al. Artificial Intelligence for teleophthalmology-based diabetic retinopathy screening in a national programme: an economic analysis modelling study. *Lancet Digit Health.* 2020;2(5):240-249. doi:10.1016/S2589-7500(20)30060-1
9. Dismuke C. Progress in examining cost-effectiveness of AI in diabetic retinopathy screening. *Lancet Digit Health.* 2020;2(5):e212-e213. doi:10.1016/S2589-7500(20)30077-7
10. Leavitt JA, Larson TA, Hodge DO, Gullerud RE. The incidence of central retinal artery occlusion in Olmsted County, Minnesota. *Am J Ophthalmol.* 2011;152(5):820-823. doi:10.1016/j.ajo.2011.05.005
11. Song P, Xu Y, Zha M, Zhang Y, Rudan I. Global epidemiology of retinal vein occlusion: a systematic review and meta-analysis of prevalence, incidence, and risk factors. *J Glob Health.* 2019;9(1):010427. doi:10.7189/jogh.09.010427
12. Ponto KA, Elbaz H, Peto T, et al. Prevalence and risk factors of retinal vein occlusion: the Gutenberg health study. *J Thromb Haemost.* 2015;13(7):1254-1263. doi:10.1111/jth.12982
13. Frederiksen KH, Stokholm L, Frederiksen PH, et al. Cardiovascular morbidity and all-cause mortality in patients with retinal vein occlusion: a Danish nationwide cohort study. *Br J Ophthalmol.* 2023;107(9):1324-1330. doi:10.1136/bjophthalmol-2022-321225

Archives of
Ophthalmological Research

Original Article

DOI: 10.51271/AOR-0057

Regional histopathologic differences between nasal and temporal upper eyelid tissues in blepharoplasty specimens

Elmas Yüksel Şükün*[1], Sibel Sipahioğlu[1], Işıl Çiçekdağı[2]

[1]Department of Ophthalmology, Alanya Training and Research Hospital, Antalya, Turkiye

[2]Department of Medical Pathology, Alanya Training and Research Hospital, Antalya, Turkiye

Cite this article: Yüksel Şükün E, Sipahioğlu S, Çiçekdağı I. Regional histopathologic differences between nasal and temporal upper eyelid tissues in blepharoplasty specimens. *Arch Ophthalmol Res.* 2026;3(3):57-60. doi:10.51271/AOR-0057

Received: 12/08/2026 ◆ **Accepted:** 21/09/2026 ◆ **Published:** 24/09/2026

ABSTRACT

Aims: To investigate histopathologic differences between the nasal and temporal portions of upper eyelid blepharoplasty specimens in dermatochalasis.

Methods: This retrospective observational study included 82 eyes with available nasal and temporal upper eyelid excision specimens. The number of dilated lymphatic vessels, maximum lymphatic vessel diameter, elastic fiber count, macrophage count, and capillary count were evaluated separately in both regions. Paired comparisons were performed using the paired-samples t-test or Wilcoxon signed-rank test, as appropriate.

Results: The study included 82 eyes from 41 patients. The mean age was 59.1±8.56 years; 26 patients (63.4%) were female and 15 (36.6%) were male. The nasal region showed significantly higher values for dilated lymphatic vessel count (6.99±1.79 vs 6.51±1.36; p<0.001), elastic fiber count (3.32±0.93 vs 3.06±0.91; p=0.003), and capillary count (13.46±3.14 vs 12.84±3.25; p<0.001). No significant differences were found for maximum lymphatic vessel diameter [239.29±57.71 micrometers (μm) vs 242.05±59.49 μm; p=0.228] or macrophage count (26.67±2.70 vs 26.40±2.63; p=0.101).

Conclusion: Regional histopathologic differences were observed between the nasal and temporal portions of upper eyelid blepharoplasty specimens. The nasal region showed higher counts of dilated lymphatic vessels, elastic fibers, and capillaries than the temporal region.

Keywords: Dermatochalasis, blepharoplasty, upper eyelid, histopathology, lymphatic vessels, elastic fibers

INTRODUCTION

Dermatochalasis involves histopathologic changes beyond age-related upper eyelid skin laxity, including lymphatic vessel proliferation and dilatation, stromal edema, elastic fiber loss, and macrophage accumulation.[1-3] These findings have been associated with subclinical inflammation, elastolysis, and secondary lymphostasis.[1-3] However, histopathologic studies of dermatochalasis remain limited, particularly those directly comparing different anatomic regions of the upper eyelid within the same individual.[2,3]

The upper eyelid does not behave as a clinically uniform structure. Dermatochalasis has been described as part of the broader pathophysiologic process of periorbital aging and appears to involve multilayered structural alterations beyond simple skin excess.[4,5] More recent reports have also shown that dermatochalasis may exhibit different clinical and histologic subtypes and that histopathologic changes do not necessarily follow the same pattern in all cases.[6,7] These observations suggest that histopathologic changes may vary across different regions of the upper eyelid.

Dermatochalasis may be associated not only with cosmetic concerns but also with functional symptoms.[8] Upper eyelid blepharoplasty therefore remains one of the standard surgical approaches for its treatment.[4] Against this background, identifying regional tissue differences is relevant both for understanding the pathobiology of dermatochalasis and for improving tissue characterization in blepharoplasty planning.

Given the regional differences in upper eyelid anatomy and lymphatic organization,[4,5] we hypothesized that histopathologic changes associated with dermatochalasis may not be uniformly distributed across the upper eyelid. Therefore, the present study aimed to compare nasal and temporal blepharoplasty specimens from the same eye with respect to lymphatic vessel number and diameter, elastic fiber count, macrophage count, and capillary count. We

***Corresponding Author:** Elmas Yüksel Şükün, dr.elmas.yuksel@gmail.com

hypothesized that these histopathologic parameters would differ between the nasal and temporal regions.

METHODS

Ethics

The study was approved by the Alanya Alaaddin Keykubat University Faculty of Medicine Clinical Researches Ethics Committee (Date: 01.04.2026, Decision No: 06-03) and was conducted in accordance with the principles of the Declaration of Helsinki.

Study Design

In this retrospective observational study, cases with available histopathologic evaluation of nasal and temporal upper eyelid excision specimens were reviewed. Patients were included if they had undergone upper eyelid blepharoplasty, had available tissue samples from both the nasal and temporal regions, and had complete histopathologic data. Cases with incomplete histopathologic evaluation, missing nasal or temporal specimens, or insufficient records were excluded.

Demographic data were retrieved retrospectively from medical records and pathology archives. Each eye was considered a separate unit of analysis, and right and left eyes from the same patient were analyzed as separate records. Age, gender, and histopathologic parameters were documented.

The excised upper eyelid specimens were divided into nasal and temporal portions according to anatomical landmarks. The nasal portion corresponded to the medial upper eyelid tissue between the medial limbus and the medial can thus, whereas the temporal portion corresponded to the lateral upper eyelid tissue between the lateral limbus and the lateral canthus. The specimens from the two regions were submitted separately for histopathologic examination. All tissue samples were fixed in 10% buffered formalin, embedded in paraffin, and processed according to standard histopathologic protocols.

Tissue sections were stained with hematoxylin and eosin (H&E), Masson trichrome (MT), and elastic Van Gieson (EVG). In addition, immunohistochemical staining was performed using CD68 for macrophages, D2-40 for lymphatic endothelial cells, and CD34 for vascular endothelial cells.

Statistical Analysis

Histopathologic evaluation was performed under light microscopy by the same pathologist. The following parameters were assessed separately in the nasal and temporal specimens: number of dilated lymphatic vessels, maximum lymphatic vessel diameter, elastic fiber count, macrophage count, and capillary count. The number of dilated lymphatic vessels was determined by counting D2-40-positive dilated lymphatic vessels at ×100 magnification. Maximum lymphatic vessel diameter was recorded in micrometer (μm) as the largest diameter of a lymphatic vessel identified in each specimen. Elastic fiber count was assessed using EVG staining, and the number of elastic fibers observed per 20 collagen fibers was recorded. Macrophage count was determined by counting CD68-positive cells at ×400 magnification, whereas capillary count was assessed by counting CD34-positive capillary vessels at ×400 magnification. For all parameters except maximum lymphatic vessel diameter, counts were obtained from three separate microscopic fields at the specified magnification, and the mean value was used for statistical analysis.

Statistical analyses were performed using jamovi version 2.7.6. Continuous variables were summarized as mean±standard deviation, median, and minimum and maximum values, whereas categorical variables were expressed as counts and percentages. Comparisons between the nasal and temporal regions were performed using paired analyses. Distribution of variables was assessed with the Shapiro-Wilk test. Variables with normal distribution were analyzed using the paired-samples t-test, whereas non-normally distributed paired variables were analyzed using the Wilcoxon signed-rank test. Accordingly, maximum lymphatic vessel diameter and macrophage count were analyzed using the paired-samples t-test, while the number of dilated lymphatic vessels, elastic fiber count, and capillary count were analyzed using the Wilcoxon signed-rank test. A p-value of <0.05 was considered statistically significant.

RESULTS

A total of 82 eyes from 41 patients were included in the study. The mean age of the patients was 59.1±8.56 years. Of the 41 patients, 26 (63.4%) were female and 15 (36.6%) were male.

In paired comparisons, the number of dilated lymphatic vessels was significantly higher in the nasal than in the temporal region (6.99±1.79 vs 6.51±1.36, $p<0.001$). Elastic fiber count (3.32±0.93 vs 3.06±0.91, $p=0.003$) and capillary count (13.46±3.14 vs 12.84±3.25, $p<0.001$) were also significantly higher in the nasal region. In contrast, no significant differences were observed between the nasal and temporal regions in maximum lymphatic vessel diameter (239.29±57.71 μm vs 242.05±59.49 μm, $p=0.228$) or macrophage count (26.67±2.70 vs 26.40±2.63, $p=0.101$) (Table).

DISCUSSION

In the present study, the nasal and temporal portions of upper eyelid blepharoplasty specimens were directly compared within the same eye. The nasal region showed significantly higher numbers of dilated lymphatic vessels, elastic fibers, and capillaries than the temporal region. In contrast, no significant differences were found between the two regions with respect to maximum lymphatic vessel diameter or macrophage count.

Table. Comparison of histopathologic parameters between the nasal and temporal upper eyelid regions

Variable	Nasal, mean±SD	Temporal, mean±SD	Test	p-value
Dilated lymphatic vessel count	6.99±1.79	6.51±1.36	Wilcoxon signed-rank test	<0.001
Maximum lymphatic vessel diameter (μm)	239.29±57.71	242.05±59.49	Paired-samples t-test	0.228
Elastic fiber count	3.32±0.93	3.06±0.91	Wilcoxon signed-rank test	0.003
Macrophage count	26.67±2.70	26.40±2.63	Paired-samples t-test	0.101
Capillary count	13.46±3.14	12.84±3.25	Wilcoxon signed-rank test	<0.001

Patient characteristics: 41 patients (82 eyes); mean age, 59.1±8.56 years; female, n=26 (63.4%); male, n=15 (36.6%). SD: Standard deviation, μm: Micrometer

These findings demonstrate region-specific histopathologic differences within the examined upper eyelid specimens.

Previous studies have shown that dermatochalasis cannot be explained solely by age-related tissue laxity. Nagi et al.[1] and Karnaz et al.[2] described increased lymphatic vessel density and dilatation, loss of elastic fibers, stromal edema, and increased macrophage infiltration. Kashkouli et al.[3] likewise emphasized lymphangiectasia and lymphatic dilatation as recurring histopathologic features of dermatochalasis. However, previous studies have mainly compared dermatochalasis with control tissue or examined age-related differences, whereas region-specific histopathologic comparisons within the upper eyelid remain limited.[3,7] Our finding of higher lymphatic vessel and capillary counts in the nasal region suggests that these microvascular and lymphatic alterations may not be evenly distributed throughout the upper eyelid.

In our study, no significant difference was found between the nasal and temporal regions regarding maximum lymphatic vessel diameter. Kashkouli et al.[3] reported that most histopathologic parameters were similar across age groups, with the exception of lymphatic vessel diameter, which increased with age. Within the studied specimens, the regional difference was observed in lymphatic vessel number rather than maximum vessel diameter. Previous anatomical studies have also demonstrated regional organization of upper eyelid lymphatics.[9,10]

The higher elastic fiber count in the nasal region is also noteworthy. Although previous studies reported elastic fiber loss in dermatochalasis,[1-3] these observations were largely based on comparisons between dermatochalasis specimens and control tissue. In contrast, our study compared two anatomic regions within the same eyelid and therefore indicates not an absolute excess of elastic fibers in the nasal region, but rather a relatively higher elastic fiber count compared with the temporal region. Likewise, the higher capillary count in the nasal region may indicate a more pronounced microvascular difference in this compartment. However, studies directly examining regional variation in capillary distribution within the upper eyelid remain limited.

No significant difference in macrophage count was found between the nasal and temporal regions. Although previous control-based studies have reported increased macrophage infiltration in dermatochalasis tissue,[1,2] our results did not demonstrate a regional difference within the same eyelid. This may indicate that inflammatory cellular involvement represents a general histopathologic component of dermatochalasis rather than a distinctly region-specific change.

The regional differences observed in our study demonstrate histopathologic variation between the nasal and temporal portions of the examined blepharoplasty specimens. Recent studies examining orbicularis oculi muscle alterations and systemic vitamin D status further suggest that different structural and systemic factors may be associated with dermatochalasis.[11,12] You et al.[7] identified different clinical and histologic subtypes of senile dermatochalasis and demonstrated variation in histopathologic patterns among cases. Similarly, Aydemir et al.[6] investigated the relationship between histopathologic findings and systemic biochemical status, suggesting that dermatochalasis may have heterogeneous biological determinants.

Limitations

This study has several limitations. First, its retrospective design should be acknowledged. Second, both eyes of each patient were analyzed separately, although fellow eyes are not statistically independent. The lack of adjustment for within-subject correlation should therefore be considered when interpreting the results. In addition, the dimensions of the nasal and temporal specimens were not systematically recorded; therefore, potential differences in specimen size between the two regions could not be accounted for. Furthermore, only selected histopathologic parameters were evaluated, whereas collagen stromal bed depth, intrafibrillar edema, and other immunohistochemical markers were not assessed. The absence of a control group also means that the present findings reflect regional differences rather than the full spectrum of pathologic changes associated with dermatochalasis. Dermatochalasis severity was not systematically graded; therefore, its potential association with the histopathologic findings could not be evaluated. Potential confounding factors such as skin type, smoking status, cumulative sun exposure, systemic diseases, and other environmental factors were not systematically available and therefore could not be accounted for in the analyses. On the other hand, direct comparison of nasal and temporal regions within the same eye represents an important strength of the study.

CONCLUSION

As a result, among the blepharoplasty specimens examined in this study, the nasal upper eyelid region showed higher numbers of dilated lymphatic vessels, elastic fibers, and capillaries than the temporal region, whereas maximum lymphatic vessel diameter and macrophage count did not differ significantly. These findings demonstrate regional histopathologic differences between the nasal and temporal portions of the examined upper eyelid specimens. Further prospective studies incorporating standardized specimen measurements, dermatochalasis grading, and appropriate control groups are needed to determine the clinical and pathophysiological significance of these findings.

ETHICAL DECLARATIONS

Ethics Committee Approval

This study was approved by the Alanya Alaaddin Keykubat University Faculty of Medicine Clinical Researches Ethics Committee (Date: 01.04.2026, Decision No: 06-03).

Informed Consent

This retrospective study used pre-existing anonymized patient data. No additional intervention was performed, and there was no direct patient contact. The study was approved by the Ethics Committee, and the requirement for written informed consent was waived by the ethics committee.

Peer Review Process

This manuscript was subject to external peer review.

Conflict of Interest

The authors declare no conflicts of interest related to this study.

Financial Disclosure

The authors received no financial support for the conduct or publication of this research.

Author Contributions

Concept: EYŞ, SS; Design: EYŞ, SS; Control: SS, IÇ; Data Collection and/or Processing: EYŞ, IÇ; Analysis and/or Interpretation: EYŞ, SS, IÇ; Literature Review: EYŞ; Writing the Article: EYŞ; Critical Review: EYŞ, SS, IÇ.

REFERENCES

1. Nagi KS, Carlson JA, Wladis EJ. Histologic assessment of dermatochalasis: elastolysis and lymphostasis are fundamental and interrelated findings. *Ophthalmology.* 2011;118(6):1205-1210. doi:10.1016/j.ophtha.2010.10.013
2. Karnaz A, Katircioglu YA, Ozdemir ES, Celebli P, Hucumenoglu S, Ornek F. The histopathological findings of patients who underwent blepharoplasty due to dermatochalasis. *Semin Ophthalmol.* 2018;33(3):407-411. doi:10.1080/08820538.2017.1282970
3. Kashkouli MB, Karimi N, Johari-Moghadam MM, Shayanfar N, Aghamirsalim M, Abdolalizadeh P. Dermatochalasis through decades: a histopathologic study. *Ann Plast Surg.* 2021;86(3):340-344. doi:10.1097/SAP.0000000000002489
4. Bhattacharjee K, Misra D, Deori N. Updates on upper eyelid blepharoplasty. *Indian J Ophthalmol.* 2017;65(7):551-558. doi:10.4103/ijo.IJO_540_17
5. De Biasio F, Miotti G, Zingaretti N, Castriotta L, Parodi PC. Study on the aging dynamics of the periorbital region: from observation to knowledge of physiopathology. *Ophthalmic Plast Reconstr Surg.* 2019;35(4):333-341. doi:10.1097/IOP.0000000000001247
6. Aydemir E, Malkoç Şen E, Aksoy Aydemir G, Bayat AH, Karnaz A, Aydın Türk B. Relationship between histopathological findings of patients with dermatochalasis and vitamin D deficiency. *Int Ophthalmol.* 2024;44(1):285. doi:10.1007/s10792-024-03209-3
7. You H, Kim G, Lew H. A novel classification of senile dermatochalasis: insights from clinical and histological analysis. *Graefes Arch Clin Exp Ophthalmol.* 2024;262(8):2643-2649. doi:10.1007/s00417-024-06430-z
8. Avisar I, Norris JH, Selva D, Malhotra R. Upper-eyelid wick syndrome: association of upper-eyelid dermatochalasis and tearing. *Arch Ophthalmol.* 2012;130(8):1007-1012. doi:10.1001/archophthalmol.2012.1340
9. Wu G, Yang Y, Sheng L, et al. Eyelid lymphatics: an anatomical study by microdissection. *J Craniofac Surg.* 2021;32(8):2878-2882. doi:10.1097/SCS.0000000000007759
10. Nishioka H, Takashimizu I, Yuzuriha S. Upper eyelid lymphatic anatomy is associated with blepharoplasty recovery. *J Plast Reconstr Aesthet Surg.* 2024;99:248-255. doi:10.1016/j.bjps.2024.09.079
11. Krajewska-Węglewicz L, Felczak P, Adamek D, Dorobek M. Damage to the orbicularis oculi muscle may impair the development of dermatochalasis. *Sci Rep.* 2024;14(1):2417. doi:10.1038/s41598-024-52955-y
12. Seyyar SA, Tokuc EO. Evaluation of 25-hydroxyvitamin D levels in patients with dermatochalasis. *Int Ophthalmol.* 2023;43(3):749-756. doi:10.1007/s10792-022-02474-4

Archives of
Ophthalmological Research

Original Article

DOI: 10.51271/AOR-0058

Subfoveal suprachoroidal space and choroidal thickness changes after a near-vision task in healthy young adults

Yusuf Evcimen*, İffet Yarımağa, Mustafa Güleşce
Department of Ophthalmology, Van Training and Research Hospital, Van, Turkiye

Cite this article: Evcimen Y, Yarımağa İ, Güleşce M. Subfoveal suprachoroidal space and choroidal thickness changes after a near-vision task in healthy young adults. *Arch Ophthalmol Res.* 2026;3(3):61-65. doi:10.51271/AOR-0058

Received: 20/08/2026 ◆ **Accepted:** 21/09/2026 ◆ **Published:** 24/09/2026

ABSTRACT

Aims: To evaluate subfoveal suprachoroidal space (SCS) and choroidal thickness (ChT) changes immediately after a near-vision task.

Methods: This prospective within-subject before-and-after study included one eye from each of 74 healthy adults aged 18-40 years. After 5 minutes of seated rest, a baseline structural macular optical coherence tomography scan was obtained. Participants then completed a 3-minute near-vision task using a high-contrast target at 33 cm, and the scan was repeated immediately after the task. SCS and choroidal thicknesses were measured by two masked graders. The primary outcome was within-eye SCS thickness change from baseline, assessed with a paired t-test. Choroidal thickness change and the Pearson correlation between changes in the two thickness measurements were also evaluated.

Results: The study included 74 participants (36 male and 38 female) with a mean age of 28.6±6.4 years. SCS thickness increased from 29.8±6.8 to 41.2±8.9 µm (mean change, +11.4 µm; 95% CI, 10.6-12.3 µm; p<.001). ChT decreased from 258.4±64.2 to 231.6±58.8 µm. ΔChT and ΔSCS were negatively correlated (r=-0.64; 95% CI, -0.76 to -0.48; p<.001). The visible-SCS subgroup (n=65) showed a similar correlation (r=-0.65).

Conclusion: The post-task SCS increase and ChT decrease were negatively correlated. These exploratory associations do not establish mechanical coupling or volume redistribution.

Keywords: Accommodation, near work, suprachoroidal space, choroidal thickness, optical coherence tomography

INTRODUCTION

Near viewing increases accommodative demand and is accompanied by ciliary muscle contraction, convergence, pupillary constriction, and small changes in posterior ocular biometry. Controlled optical-stimulus and sustained near-work studies have reported changes in axial length and choroidal thickness (ChT), although their magnitude depends on stimulus strength, task duration, refractive correction, and image-acquisition timing.[1,2]

The suprachoroidal space (SCS) lies between the choroid and sclera and contributes to uveoscleral fluid pathways.[3] Enhanced-depth optical coherence tomography (OCT) can show a hyporeflective suprachoroidal layer in some healthy eyes, although visibility and measured thickness depend on age, device characteristics, image quality, and boundary definitions.[4,5] The SCS has also attracted interest as a route for posterior-segment drug delivery, making reliable description of its normal anatomy relevant.[6]

Liu and colleagues[2] evaluated choroidal metrics before and immediately after supervised near work at 33 cm, thereby separating the near-vision task from OCT acquisition. Whether the OCT-defined subfoveal SCS measurement also changes immediately after a standardized near-vision task has not been well characterized.

The principal outcome in this focused report was the paired change in subfoveal SCS thickness immediately after a 3-minute near-vision task in adults aged 18-40 years. Secondary exploratory outcomes were the paired change in subfoveal ChT and the association between ΔChT and ΔSCS.

METHODS

Ethics

The protocol was approved by the Van Training and Research Hospital Non-interventional Clinical Researches Ethics Committee (Date: 03.04.2026, Decision No: GOKAEK/2026-04-03), and written informed consent was obtained from all

***Corresponding Author:** Yusuf Evcimen, yusufevcimen23@gmail.com

participants. Recruitment, consent, and all research-specific procedures began after ethics approval. The study adhered to the principles of the Declaration of Helsinki.

Study Design and Participants

This prospective within-subject before-and-after study was conducted in the Department of Ophthalmology of a tertiary training and research hospital.

Seventy-four eligible participants aged 18-40 years were enrolled after ethics approval. One eye per participant was included; when both eyes were eligible, the right eye was selected to avoid within-participant inter-eye dependence.

Eligibility criteria were best-corrected visual acuity (BCVA) of 1.0 decimal (0.00 logMAR; 20/20), spherical equivalent between -6.00 and +3.00 diopters, astigmatism less than 1.50 diopters, clear ocular media, and no ocular disease on examination. Refractive error was not an exclusion criterion within these limits; appropriate spectacle correction was worn during the near-vision task. Exclusion criteria were previous ocular surgery, systemic disease or medication likely to influence ciliary muscle function or choroidal physiology, contact-lens wear within 72 hours, pregnancy or breastfeeding, inability to complete imaging, or inadequate OCT image quality. Participants were asked to avoid caffeine, alcohol, tobacco, and strenuous exercise for 12 hours before imaging.

Ocular Assessment and Near-Vision Protocol

All examinations were performed between 9:00 AM and 12:00 PM. Baseline evaluation included refraction, best-corrected visual acuity, slit-lamp examination, Goldmann applanation tonometry, and optical biometry with the Lenstar LS 900 (Haag-Streit AG, Koeniz, Switzerland). Structural OCT was obtained with the SOLIX spectral-domain OCT system (Optovue Inc., Fremont, CA, USA; axial resolution approximately 5 µm). No mydriatic or cycloplegic agent was administered before the OCT measurements, and dilated fundus examination was not performed as part of the study visit.

After 5 minutes of seated rest, participants were positioned at the OCT device and a baseline foveal B-scan was acquired without spectacles. Participants then viewed a high-contrast, 6/6-equivalent near target at 33 cm for 3 minutes while wearing spectacles correcting their distance refractive error and were instructed to maintain clear, single vision. Immediately after task completion, the spectacles were removed, participants were repositioned at the OCT device, and a second foveal B-scan was acquired. Thus, both OCT measurements were performed without spectacles, whereas the intervening near-vision task was performed with spectacle correction. OCT was acquired after the task rather than simultaneously with near viewing. This acquisition sequence follows the post-near-work approach described by Liu and colleagues,[2] while retaining the 3-minute task used in the present study. The target distance represented a nominal 3.0 D accommodative stimulus; the accommodative response was not objectively quantified.

Image Analysis

Baseline and immediate post-task B-scans were de-identified and graded independently by two experienced observers masked to image condition. A senior grader adjudicated discrepancies greater than 5 µm. The outer choroidal boundary was identified at the transition from hyporeflective choroidal vasculature to the more homogeneous hyperreflective sclera. Subfoveal ChT was defined as the distance from the outer retinal pigment epithelium (RPE) border to this choroidal boundary. SCS thickness was defined as the distance from the outer choroidal boundary to the inner scleral surface. Both measurements were made at the foveal center on the same baseline and post-task B-scans using the built-in digital caliper. These definitions treat ChT and SCS thickness as adjacent measurements with a shared boundary.

A distinct hyporeflective SCS band was recorded as visible or non-visible. When no distinct band was visible, the minimum separation between the outer choroidal stroma and inner scleral surface was recorded. Because this surrogate may not represent the same anatomical construct as a visible SCS band, sensitivity results for both the SCS change and the ΔChT-ΔSCS association are presented for eyes with a visible band.

Intergrader agreement was estimated with a two-way random-effects intraclass correlation coefficient for absolute agreement. Intragrader agreement was assessed when the senior grader repeated measurements from 40 stored scans after 2 weeks. These analyses quantify grader-related segmentation agreement on the same images; they do not estimate test-retest acquisition variability.[7]

Statistical Analysis

Continuous variables were expressed as mean±standard deviation (SD), and categorical variables as counts and percentages. Within-eye change (Δ) was defined as immediate post-task minus baseline. The primary outcome was subfoveal SCS thickness change. ChT change and the ΔChT-ΔSCS association were exploratory secondary outcomes.

SCS change estimates were calculated from subgroup sample sizes, mean within-eye changes, and corresponding SDs. The overall mean and variance incorporated both within-subgroup and between-subgroup variation. Paired t statistics and 95% confidence intervals (CIs) were calculated for SCS change. Differences between the visible-SCS and non-visible-SCS subgroups were evaluated using Welch's t-test.

ChT changes were presented using the available paired mean difference, 95% CI, and p-value. The association between ΔChT and ΔSCS was expressed using Pearson's correlation coefficient. Correlation CIs were calculated using Fisher's z transformation, and two-sided p-values were derived from the coefficients and sample sizes. A sensitivity analysis was restricted to eyes with a visible SCS.

All secondary analyses were exploratory, without adjustment for multiple comparisons. Individual-level data were not reanalyzed, so distributional assumptions and the influence of outliers could not be reassessed.

RESULTS

Participant Characteristics

Seventy-four participants (36 male and 38 female) were included. Mean age was 28.6±6.4 years, mean spherical equivalent was -1.18±1.88 diopters, and mean axial length was 23.7±1.0 mm (**Table 1**).

Table 1. Demographic and baseline ocular characteristics (n=74)

Parameter	Mean±SD or n (%)	Range
Age, years	28.6±6.4	18-40
Gender, male/female	36 (48.6)/38 (51.4)	-
Spherical equivalent, D	-1.18±1.88	-5.88 to +2.96
Axial length, mm	23.7±1.0	21.9-26.2
Baseline intraocular pressure, mmHg	13.0±3.8	6.0-22.0
Baseline subfoveal SCS thickness, µm	29.8±6.8	3.2-46.8
Baseline subfoveal ChT, µm	258.4±64.2	112.6-468.3

Values are retained from the reported cohort summaries. SD: Standard deviation, D: Diopters, SCS: Suprachoroidal space, ChT: Choroidal thickness

Subfoveal Suprachoroidal Space (SCS) Thickness

Mean subfoveal SCS thickness increased from 29.8±6.8 µm at baseline to 41.2±8.9 µm immediately after the 3-minute near-vision task. The paired mean change was +11.4±3.7 µm (95% CI, 10.6-12.3 µm; p<.001). An increase occurred in 70 of 74 eyes (94.6%) (Table 2; Figure 1A).

Table 2. Subfoveal SCS and choroidal thickness before and immediately after the 3-minute near-vision task (n=74)

Measure	Baseline mean±SD	Post-task mean±SD	Mean paired change	95% CI of change	p-value
SCS thickness	29.8±6.8	41.2±8.9	+11.4	10.6 to 12.3	<.001
ChT	258.4±64.2	231.6±58.8	-26.8	-31.2 to -22.4	<.001

All thickness values and changes are in µm. Change=Immediate post-task-baseline. SCS change statistics were estimated from rounded subgroup summaries; ChT results were retained from the original analysis. SCS: Suprachoroidal space, SD: Standard deviation, CI: Confidence interval, ChT: Choroidal thickness

A distinct hyporeflective SCS band was visible in 65 eyes (87.8%); a minimum-separation surrogate was used in the remaining 9 eyes. Mean changes were +11.6±3.7 µm in the visible-SCS subgroup (95% CI, 10.7-12.5 µm; p<.001) and +10.2±3.2 µm in the non-visible subgroup. The between-subgroup difference was 1.4 µm (95% CI, -1.2 to 4.0 µm; p=.25). This comparison does not establish equivalence between the two measurement approaches.

Intergrader and intragrader intraclass correlation coefficients for SCS measurements on stored images were 0.96 (95% CI, 0.94-0.98) and 0.97 (95% CI, 0.95-0.98), respectively. For ChT, both coefficients were 0.98 (95% CI, 0.97-0.99).

Subfoveal Choroidal Thickness

Reported mean subfoveal ChT decreased from 258.4±64.2 µm at baseline to 231.6±58.8 µm immediately after the task (mean paired change, -26.8 µm; reported 95% CI, -31.2 to -22.4 µm; p<.001). A decrease was reported in 68 of 74 eyes (91.9%) (Table 2; Figure 1B).

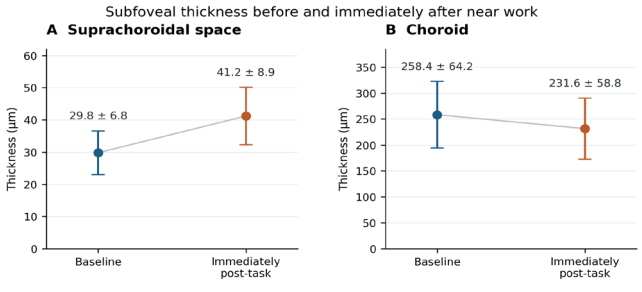

Figure 1. Subfoveal thickness of the suprachoroidal space (A) and choroid (B) before and immediately after the near-vision task (74 eyes). Points and error bars show mean±SD; lines connect group means. Panels use different vertical scales

SD: Standard deviation

Association Between ΔChT and ΔSCS

The reported correlation between subfoveal ΔChT and ΔSCS was r=-0.64. The approximate Fisher 95% CI calculated from r and n=74 was -0.76 to -0.48 (p<.001). Thus, larger SCS increases were associated with more negative ChT changes. In the reported analysis restricted to 65 eyes with a visible SCS band, r was -0.65 (approximate 95% CI, -0.77 to -0.48; p<.001) (Table 3; Figure 2). These coefficients describe association and do not quantify transfer of tissue or fluid between compartments.

Table 3. Association between within-eye changes in subfoveal ChT and SCS thickness

Analysis set	n	Pearson r	Approximate 95% CI	p-value
All eyes	74	-0.64	-0.76 to -0.48	<.001
Visible SCS only	65	-0.65	-0.77 to -0.48	<.001

Δ=Immediate post-task-baseline. Approximate CIs and p-values were calculated from reported r and n. The visible-SCS subgroup is included in the full cohort. ChT: Choroidal thickness, SCS: Suprachoroidal space, CI: Confidence interval

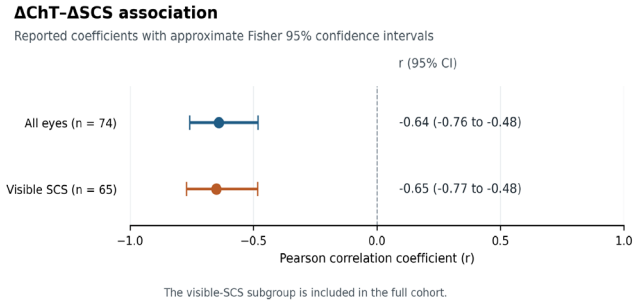

Figure 2. Correlation between changes in subfoveal ChT (ΔChT) and SCS thickness (ΔSCS). Points and bars show reported Pearson r and approximate 95% CIs for the full cohort (74 eyes) and its visible-SCS subgroup (65 eyes)

Δ=Immediate post-task-baseline, ChT: Choroidal thickness, SCS: Suprachoroidal space, CI: Confidence interval

DISCUSSION

Subfoveal SCS thickness increased and ChT decreased immediately after the 3-minute near-vision task, with mean changes of +11.4 µm and -26.8 µm, respectively. The within-eye changes were negatively correlated (r=-0.64), and a similar association was present in eyes with a visible SCS band. These observations describe a post-task association but do not identify the physiological pathway responsible for it.

Woodman-Pieterse and colleagues[1] observed choroidal thinning during a 6-D accommodative stimulus, whereas Liu and colleagues[2] acquired OCT after near work and found a mean subfoveal ChT decrease of 5.1 µm after 20 minutes in myopic adults. The direction of the ChT change in the present study is consistent with these observations, but its magnitude was greater despite the shorter task. Differences in stimulus duration, refractive characteristics, imaging platform, boundary definitions, and acquisition timing limit direct comparison. The shared direction of change does not validate the magnitude observed here; independent replication is needed.

Possible explanations for the post-task changes include ciliary muscle-related mechanical effects on the choroid and sclera, convergence-related forces, and autonomic or vascular responses to near viewing.[8,9] The 33-cm target provided a nominal accommodative stimulus, but the actual response was not measured. Because OCT was obtained after task completion, the observations may reflect residual

or recovering responses and cannot be interpreted as direct measurements during sustained accommodation.

Başkan and colleagues[10] reported an association between greater IOP increases and greater choroidal thinning following cervical flexion in healthy adults. Ha and colleagues[11] also reported transient IOP elevation during smartphone-based near work, with larger increases associated with greater neck flexion. These findings raise the possibility that an IOP rise accompanying near work could contribute to choroidal thinning. However, the exposures differed from the present task, and neither post-task IOP nor neck position was included in our analysis. A pressure-related contribution therefore remains a hypothesis; an IOP increase in this cohort cannot be assumed.

The negative ΔChT-ΔSCS correlation also requires caution because the measurements share the outer choroidal boundary. Placing this boundary more anteriorly decreases measured ChT and increases measured SCS thickness, even if the RPE and inner scleral positions are unchanged. Correlated boundary-placement errors could therefore contribute to the inverse association. Restricting the analysis to eyes with a visible SCS band does not remove this dependence. The correlation and the changes in linear thickness do not establish fluid transfer, mechanical coupling, or volume redistribution between compartments.

The SCS band was visible in 87.8% of eyes, compared with 44.6% in the cohort studied by Yiu and colleagues.[4] Differences in the study populations, imaging platforms, and boundary criteria limit direct comparison of these proportions. The positive SCS change in the visible-band subgroup indicates that the overall finding was not confined to surrogate measurements. Nevertheless, the small non-visible subgroup and the non-significant between-subgroup comparison do not establish that minimum separation and visible-band thickness represent equivalent anatomical measurements.

Strengths include the use of one eye per participant, within-eye comparisons, a morning examination window, a fixed task duration and target distance, and masked grading. The high agreement on stored scans supports consistency between readers, in keeping with work on manual choroidal thickness measurement.[7] These features improve comparability, but grader agreement does not quantify variability introduced by acquiring a new scan.

Limitations

The principal limitations are the absence of objective accommodation measurements, a single post-task assessment, the lack of a time-matched control and independent repeat acquisitions, manual boundary identification, and use of a surrogate when the SCS band was not visible. Spectacle removal and repositioning introduced a task-to-scan delay that was not quantified. Although the intended sequence was immediate post-task imaging, its exact latency was not established and may have influenced the measurements. The single-center, young-adult sample also limits generalizability.

Individual-level data were not reanalyzed, so data consistency, distributional assumptions, and influential observations could not be independently assessed. The paired ChT CI and p-value were not independently recalculated. Secondary analyses were exploratory, with no adjustment for multiple comparisons. The findings should therefore be considered hypothesis-generating and do not establish normative values or clinical applications.

CONCLUSION

Subfoveal SCS thickness increased and ChT decreased after the 3-minute near-vision task, and the within-eye changes were negatively correlated. The association does not distinguish physiological coupling from shared-boundary measurement effects or other influences accompanying near work. Confirmation requires verification against individual-level measurements, objective assessment of accommodation and IOP, documented task-to-scan timing, independent repeat acquisitions, and a time-matched control condition.

ETHICAL DECLARATIONS

Ethics Committee Approval

This study was approved by the Van Training and Research Hospital Non-interventional Clinical Researches Ethics Committee (Date: 03.04.2026, Decision No: GOKAEK/ 2026-04-03).

Informed Consent

Written informed consent was obtained from all individual participants prior to their inclusion in the study. Participants were fully informed about the study's aims, procedures, potential risks and benefits, and their rights-including the right to withdraw at any time without consequence. All participants voluntarily signed a written informed consent form.

Peer Review Process

This manuscript was subject to external peer review.

Conflict of Interest

The authors declare no conflicts of interest related to this study.

Financial Disclosure

The authors received no financial support for the conduct or publication of this research.

Author Contributions

Concept: YE; Design: YE; Control: YE; Resources: YE, İY; Materials: YE; Data Collection and/or Processing: YE; Analysis and/or Interpretation: YE; Literature Review: İY; Writing the Article: İY, MG; Critical Review: İY.

Acknowledgments

The authors thank the nursing and imaging staff of Van Training and Research Hospital.

REFERENCES

1. Woodman-Pieterse EC, Read SA, Collins MJ, Alonso-Caneiro D. Regional changes in choroidal thickness associated with accommodation. *Invest Ophthalmol Vis Sci.* 2015;56(11):6414-6422. doi:10.1167/iovs.15-17102
2. Liu M, Wang Y, Li H, et al. Differences in choroidal responses to near work between myopic children and young adults. *Eye Vis (Lond).* 2024;11(1):12. doi:10.1186/s40662-024-00382-5
3. Krohn J, Bertelsen T. Corrosion casts of the suprachoroidal space and uveoscleral drainage routes in the human eye. *Acta Ophthalmol Scand.* 1997;75(1):32-35. doi:10.1111/j.1600-0420.1997.tb00245.x
4. Yiu G, Pecen P, Sarin N, et al. Characterization of the choroid-scleral junction and suprachoroidal layer in healthy individuals on enhanced-depth imaging optical coherence tomography. *JAMA Ophthalmol.* 2014;132(2):174-181. doi:10.1001/jamaophthalmol.2013.7288

5. Spaide RF, Koizumi H, Pozzoni MC. Enhanced depth imaging spectral-domain optical coherence tomography. *Am J Ophthalmol.* 2008;146(4):496-500. doi:10.1016/j.ajo.2008.05.032
6. Chiang B, Jung JH, Prausnitz MR. The suprachoroidal space as a route of administration to the posterior segment of the eye. *Adv Drug Deliv Rev.* 2018;126:58-66. doi:10.1016/j.addr.2018.03.001
7. Rahman W, Chen FK, Yeoh J, Patel P, Tufail A, Da Cruz L. Repeatability of manual subfoveal choroidal thickness measurements in healthy subjects using the technique of enhanced depth imaging optical coherence tomography. *Invest Ophthalmol Vis Sci.* 2011;52(5):2267-2271. doi:10.1167/iovs.10-6024
8. Croft MA, Nork TM, McDonald JP, Katz A, Lutjen-Drecoll E, Kaufman PL. Accommodative movements of the vitreous membrane, choroid, and sclera in young and presbyopic human and nonhuman primate eyes. *Invest Ophthalmol Vis Sci.* 2013;54(7):5049-5058. doi:10.1167/iovs.12-10847
9. Nickla DL, Wallman J. The multifunctional choroid. *Prog Retin Eye Res.* 2010;29(2):144-168. doi:10.1016/j.preteyeres.2009.12.002
10. Başkan B, Evcimen Y, Yarımağa İ, Ayyürek F. Acute effects of standardized cervical flexion on intraocular pressure, choroidal thickness, and peripapillary capillary density: a prospective self-controlled study. *East J Med.* 2026;31(3):432-440. doi:10.5505/ejm.2026.53077
11. Ha A, Kim YK, Park YJ, Jeoung JW, Park KH. Intraocular pressure change during reading or writing on smartphone. *PLoS One.* 2018;13(10):e0206061. doi:10.1371/journal.pone.0206061